

Tumor and Its Stages Detection in Brain MRI Using Template Based K-means and Fuzzy C-means Clustering Algorithm

by

Rasel Ahmmed

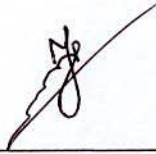
A thesis submitted in partial fulfilment of the requirements for the degree of Master of Science in Electronics and Communication Engineering



Khulna University of Engineering & Technology
Khulna-9203, Bangladesh
January, 2016

Declaration

This is to certify that the thesis work entitled "*Tumor and Its Stages Detection in Brain MRI Using Template Based K-means and Fuzzy C-means Clustering Algorithm*" has been carried out by *Rasel Ahmmed* in the Department of *Electronics and Communication Engineering*, Khulna University of Engineering & Technology (KUET), Khulna, Bangladesh. The above thesis work or any part of this work has not been submitted anywhere for the award of any degree or diploma.



Signature of Supervisor




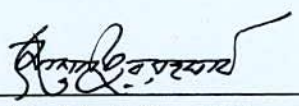
Signature of Candidate

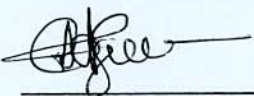
Approval


This is to certify that the thesis work submitted by *Rasel Ahmmed* entitled "*Tumor and Its Stages Detection in Brain MRI Using Template Based K-means and Fuzzy C-means Clustering Algorithm*" has been approved by the board of examiners for the partial fulfillment of the requirements for the degree of *Master of Science in Electronics and Communication Engineering (M. Sc. Eng. in ECE)*, Khulna University of Engineering & Technology (KUET), Khulna, Bangladesh in January 2016.

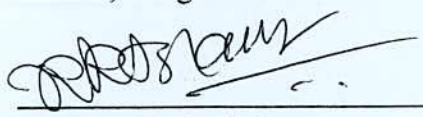
BOARD OF EXAMINERS

1. 

Dr. Md. Foisal Hossain
Associate Professor
Khulna University of Engineering & Technology (KUET)
Khulna, Bangladesh. Chairman
(Supervisor)
2. 

Prof. Dr. Mostafizur Rahman
Head of the Department
Department of Electronics and Communication Engineering
Khulna University of Engineering & Technology (KUET)
Khulna, Bangladesh. Member
3. 

Dr. A.B.M. Aowlad Hossain
Professor
Khulna University of Engineering & Technology (KUET)
Khulna, Bangladesh. Member
4. 

Dr. Shiekh Md. Rabiul Islam
Associate Professor
Khulna University of Engineering & Technology (KUET)
Khulna, Bangladesh. Member
5. 

Dr. Kazi Khairul Islam
Professor
Islamic University of Technology (IUT)
Dhaka, Bangladesh. Member
(External)

Dedicated to My Parents

Late Abdul Mannan & Mst. Papia Khatun
Those who have chosen underprivileged life to continue my smile.

Acknowledgements

First of all, I would like to bend myself to Almighty for giving me the strength and confidence to complete my thesis work, successfully.

Then I would like to acknowledge my deep gratitude to my graduation committee.

This thesis work marks an important period in my life during which many people have played an important role. Although the author's name is the only one to appear on the cover, it is the combined effort of these people that helped me to complete this research work. Therefore, I would like to take this opportunity to thank several individuals for their contributions, realizing that such a list can never be complete.

*It is a great pleasure to express my deepest gratitude and profound respect to my honourable supervisor, **Dr. Md. Faisal Hossain**, Associate Professor, Department of Electronics and Communication Engineering, KUET, who fully gave many invaluable advices, proper guidance, constant encouragement, constructive suggestions, and kind co-operation throughout the entire progress of this research work. Especially, our meetings during the last couple of months were of great support. During all those meetings, he talked with such enthusiasm about my research, presentation, publications, etc. those made it always very interesting. I enjoyed all our meetings and above all want to thank him again for all the good advices.*

*I am also so much grateful to **Prof. Dr. Md. Mostafizur Rahmman**, the honourable Head, Department of Electronics and Communication Engineering, KUET, as well as the member of this thesis examination committee, for his loving and cordial advices to prepare my thesis proposal and final thesis paper. It is also a great opportunity for me to show my gratitude and thanks to my one of the most favourite teachers, **Prof. Dr. Abdur Rafiq**, Department of Electrical and Electronic Engineering, KUET, who encouraged me, a lot, to work about this topic, when I was so confused to choose my thesis issue.*

I wish to complement to all teachers and technicians of the Department of Electronics and Communication Engineering, KUET for their co-operations and relentless encouragements in various ways throughout this work.

*Finally, it is also my duty to express gratefulness and appreciations to my respected brothers **Md. Asadur Rahman** and **Badal Banik**, as well as obviously my family members for their unswerving inspirations to complete my work.*

Rasel Ahmmed
January, 2016.

Abstract

Segmentation is obligatory process in medical application for MRI image to detect brain tumour. This research work represents a robust segmentation method which is the integration of Template based K-means and modified Fuzzy C-means (TKFCM) clustering computed algorithm that, reduces the lack of operator performance, and error in equipment. In this method, the template is selected based on convolution between grey level intensity in small portion of brain image, and brain tumour image. K-means algorithm is to emphasized initial segmentation through the proper selection of template. Updated membership of FCM is obtained through distances from cluster centroid to cluster data points, until it reaches to its best. This Euclidian distance depends upon the different features i.e. intensity, entropy, contrast, dissimilarity and homogeneity of coarse image, which was depended only on similarity in conventional FCM. Then, on the basis of updated membership and automatic cluster selection, a sharp segmented image is obtained with red marked tumour from modified FCM technique. The small deviation of grey level intensity of normal and abnormal tissue is detected through TKFCM. For the tumor and its stages classification the linearization and region properties algorithm is needed to apply on detected tumor obtained from TKFCM, which provides the characteristics parameters like area, eccentricity, bounding box, perimeters and orientation. By these parameters the classified tumor and its stages are extracted. Besides the performances of TKFCM method is analyzed through neural network not only mathematically but also graphically. The resultant values give a better regression and least error compare to the other existing methods. This method will also help in detecting tumor in multiple intensity based brain MRI image.

Contents

	PAGE
<i>Title</i>	i
<i>Declaration</i>	ii
<i>Approval</i>	iii
<i>Acknowledgement</i>	v
<i>Abstract</i>	vi
<i>Contents</i>	vii-viii
<i>List of Figures</i>	x-xi
<i>List of Tables</i>	xii
<i>List of Abbreviation</i>	xiii
CHAPTER 1 Introduction	1-7
1.1 Introduction	2
1.2 Motivation	2
1.3 Background Study	4
1.4 Challenges	5
1.5 Contribution of This Research	6
1.6 Outlines of Thesis	7
CHAPTER 2 Brain Tumors and Magnetic Resonance Imaging	8-18
2.1 Introduction	9
2.2 Brain Anatomy overview	9
2.3 Brain Tumors	11
2.4 Types of Brain Tumors	12
2.4.1 Primary Brain Tumors	12
2.4.1.1 Benign Brain Tumors	12
2.4.1.2 Malignant Brain Tumors	12
2.4.2 Metastatic Brain Tumors	13
2.5 Magnetic Resonance Imaging (MRI)	13
2.6 MRI Brain Imaging and Characteristics of Brain Tumors	16
2.7 Difficulties in Segmentation of Brain MRI	17
2.8 Summary	18

CHAPTER 3	Segmentation of Brain MRI Image	19-29
3.1	Introduction	20
3.2	Image Segmentation	20
3.2.1	Threshold Based segmentation	21
3.2.2	Edge Based Segmentation	23
3.2.3	Region Based Segmentation	24
3.2.4	Clustering Techniques	25
3.2.5	Matching	26
3.2.6	Spatial Clustering	28
3.2.7	Split and Merge Segmentation	28
3.2.8	Region Growing	28
3.3	Summary	29
CHAPTER 4	Conventional Techniques for Brain Tumor Detection	30-48
4.1	Introduction	31
4.2	Conventional Techniques for Brain Tumor Detection	31
4.2.1	Thresholding	31
4.2.2	Region Growing	34
4.2.3	Classifiers	37
4.2.4	Artificial Neural Network	39
4.2.5	Expectation Maximization	40
4.2.6	Clustering	41
4.2.6.1	K-means Clustering	41
4.2.6.2	Fuzzy C-means Clustering	43
4.3	Summary	48
CHAPTER 5	TKFCM Scheme for Tumor Detection	49-64
5.1	Introduction	50
5.2	TKFCM Algorithm for Tumor Detection	50
5.3	Results and Performance Analysis	55
5.4	Summary	64
CHAPTER 6	TKFCM Scheme for Tumor Classification	65-76
6.1	Introduction	66
6.2	TKFCM Algorithm for Tumor Classification	66
6.3	Results and Performance Analysis	70
6.4	Summary	76

CHAPTER 7 Conclusions	77-80
6.1 Outcomes	78
6.2 Limitations	79
6.3 Applications and Future Work	80
<i>References</i>	81-89
<i>List of Publications</i>	90

List of Figures

Figure No.	Description	Page
2.1	Overview structure of human brain, left side: an axial slice mr image, right side: the colour coded version of image left side	10
2.2	The major subdivision of human brain	10
2.3	Age-specific incidence rates of tumours within CNS, meninges, cranial nerves and peripheral nervous system, 2000-2004, Norway, malignant and benign	11
2.4	Brain MR images form (b) axial plane, (c) sagittal plane and (d) coronal plane	14
2.5	Original raw MRI data from Pioneer Diagnostic Center	15
2.6	Tumor region intensity characteristics	15
2.7	MRI scanner cut away	16
3.1	Basic segmentation with different criteria	21
3.2	Example of using multiple thresholds for segmentation	22
3.3	Example of edge-based segmentation	24
3.4	Example of region growing based on a grey level range	25
3.5	Finding clusters of measurement data points is often similar to image segmentation	25
3.6	Image matching based segmentation	26
3.7	Definitions for image matching	27
4.1	Thresholding based segmented brain MRI image	33
4.2	Region growing based segmentation	35
4.3	Comparison of region growing and region spilt & merge segmentation process	36
4.4	Classifier based segmented image	37
4.5	Color coded ANN based segmentation (left side) and example of ANN based brain MRI image segmentation (right side)	39
4.6	Expectation maximization based segmented image	40
4.7	K-means clustering based image segmentation	43

Figure No.	Description	Page
4.8	FCM based brain MRI tumor detection	47
5.1	The flowchart of proposed TKFCM algorithm for tumor detection	54
5.2	The database of 40 brain tumor MRI image	55
5.3	The pre-processing steps of the TKFCM,	56
5.4	Enhanced input images for TKFCM in (a & d), segmented images from the 1st segmented algorithm (Template based K-means) in (b & e), and detected brain tumor images from the TKFCM in (c & f).	57
5.5	Several clustered images for input image no. 3	58
5.6	The neural network architecture	58
5.7	The performance curve for this method through neural network	59
5.8	The validation check, minimum gradient, and Mu curve for the network	60
5.9	The error histogram curve for the network	60
5.10	The regression curve for the network	61
6.1	The flowchart of proposed TKFCM algorithm for brain tumor classification	69
6.2	The database of 30 brain tumor MRI image	70
6.3	Several clustered images for input image no. 3	71
6.4	Enhanced input images for TKFCM in (a & d), detected brain tumor images from the TKFCM in (b & e), classified brain tumor through linearization of TKFCM in (c & f)	72

List of Tables

Table No.	Description	Page
5.1	Parameters of performance analysis among conventional methods & TKFCM method	62
5.2	Comparison among the conventional methods & TKFCM method	63
5.3	Comparison of computational time among the conventional methods & TKFCM method	63
6.1	Standard area of the tumor classification	73
6.2	Calculation of characteristics parameters of tumors and classification of tumor stages	74
6.3	Comparison among the conventional methods & TKFCM method	75
6.4	Comparison of computational time among the conventional methods & TKFCM method	75

List of Abbreviation

Abbreviated form	Elaboration
CAD	Computer Aided Diagnostics
CSF	Cerebrospinal Fluid
CT	Computed Tomography
GM	Grey Matter
MRI	Magnetic Resonance Imaging
PET	Positron Emission Tomography
SPECT	Single Photon Emission Tomography
TKFCM	Template based K-means & Fuzzy C-means
WM	White Matter

CHAPTER 1

Introduction

Chapter Outlines

- ❖ Introduction
- ❖ Motivation
- ❖ Literature Review
- ❖ Challenges
- ❖ Contribution of This Research
- ❖ Outlines of Thesis

Introduction

1.1 Introduction

With the pace of civilization the growth of technology is tremendous, especially in the field of Bioscience. The human beings are always looking for the better solution of the limitation within which they are belonging. The field of advancement in computer aided diagnostic image processing; drug designing, detection and classification are one of the best examples of human limitation [1].

The human body is full of mystery and changing randomly within a fraction of time. That is a why constant output from the brain behavior which is a complicated structure is so difficult. The growth of tumor in the brain is causes an increase of drastically change which may results a sudden death. Every year a million of people are affected by brain tumor but in wants of proper detection of tumor its growth reached at dangerous condition [].

For the detection of tumor there are several imaging techniques like computed tomography (CT), magnetic resonance imaging (MRI), Doppler ultrasound, and various imaging techniques based on nuclear emission (PET (positron emission tomography), SPECT (single photon emission computed tomography), etc.) are used for brain imaging [5]. But for the complex structure of brain the gray level intensity difference is little that sometimes misleads to hilarious results.

So, a computer aided diagnostics image processing is required to mitigate this problem. The proposed method is discussed in this thesis may help the experts for better solution.

1.3 Motivation

In modern civilization the Biomedical Engineering is the emerging field of research, as it concern about the healthcare. Biomedical Engineering deals with biosignaling, bioinformatics, bioimage processing, biophotonics, biorganics etc. in point of our body. Biomedical image processing has experienced dramatic expansion, and has been an interdisciplinary research field attracting expertise from applied mathematics, computer sciences, engineering, statistics, physics, biology and medicine. Computer-aided diagnostic processing has already become an important part of clinical routine. The widespread use of computer-assisted diagnosis (CAD) can be traced back to the emergence of digital mammography in the early 1990s [1].

As if it is need not to argue that brain is our inevitable organ in our body. Any harm to any part of any small cell of brain can be dangerous to whole body. Brain is the main portion of our body, where the memory, emotion, speech, and control of whole body are centered. Therefore, abnormal cell division or growing tumor causes miscellaneous problems to the malfunction of our body, even for the muscle and eyebrow movement [2]. The tumor can paralyze the major areas of brain. There are two categories of brain tumor like- (a) Benign and (b) Malignant [3]. The first one behaves like a normal tissue which does not spread. But the last one has four stages such as- i) stage I- tissue area is like normal tumor which just congested in an area, ii) stage II- tumor with or without lymph node but not enough spreading, iii) stage III- tumor fixed or spread enough above collarbone, and iv) stage IV- tumors are spread to other parts (metastasis) of body [4].

During the past few decades, with the increasing availability of relatively inexpensive computational resources, computed tomography (CT), magnetic resonance imaging (MRI), Doppler ultrasound, and various imaging techniques based on nuclear emission (PET (positron emission tomography), SPECT (single photon emission computed tomography), etc.) have all been valuable additions to the radiologist's arsenal of imaging tools toward ever more reliable detection and diagnosis of disease. Tomographic imaging principles are rooted in physics, mathematics, computer science, and engineering [5]. Among the aforementioned imaging techniques magnetic resonance imaging (MRI) is gold accepted truthful modality in which the brain is properly imaged without any harm.

In MRI technique, brain is imaged on the basis of density of water in soft tissue of brain which is higher compared to other tissues such as bone [6]. Due to the inhomogeneity of brain structure their contrast value differs randomly in MRI, so the proper detection of tumor or tumor stages is quite difficult for the general observer [7]. In recent decades, efficient detection of brain tumor or tumor stages is being stupendous challenge for medical science. Especially for Magnetic Resonance Imaging (MRI), it is quite concerning content, as the MRI image rarely color image. Though MRI imaging technique has good contrast value over different technique, an appropriate segmentation of brain MRI image is apparent for detecting abnormality in brain. As brain comprehends complicated structure so segmentation of MRI image obliges good care and should be precise [8]. Segmentation describes salient image regions to procure region(s) of interest

(ROI's) such as lesions, tumors, edema, and necrotic tissues in brain image [9]. So, proper segmentation helps to detect tumor and tumor stages in brain MRI image.

1.2 Literature Review

For brain image segmentation numerous image processing techniques have been proposed, for example- region growing, thresholding, classifiers, Artificial Neural Networking (ANN), clustering, and so on.

Segmentation of scalar images by creating a binary partition of the image intensities is done based on thresholding. Due to structure complexity of brain tissue, proper threshold value is very hard to achieve. The main drawback of thresholding is that, it cannot be applicable for multiple channel images. In addition, it does not provide spatial characteristics, which causes it to be sensitive to noise as well as inhomogeneity intensity [10]. On the other hand, foundation of restricting threshold is also used collectively [11-12] with other methods such as classifier, ANN, clustering etc. Based on some predefined criteria *i.e.* intensity information and/or edges, the connected region of an image is extracted in region growing. [13]. Besides, the precise anatomical information is needed to locate single or multiple seed pixels for each region and together with their associated homogeneity refers as region growing [14–16]. The primary limitation in the region growing is that its seed point is found through manual interaction. In the classifier method, it needs a perfect pixel classifier for training data. Inefficient training data and classifier are aimed to time consumption and hilarious results [10]. In the clustering technique, Fuzzy c-means (FCM) clustering and expectation–maximization (EM) algorithms are being the most widely used methods for clustering [6]. The applications of the EM algorithm to brain MR image segmentation and a common disadvantage of EM algorithms are reported Wells et al. An ANN is used Hall et al, and compared the performance with FCM for segmenting brain MR images. There is a FCM algorithm which contacts with a knowledge-based classification and tissue labeling used Li et al. Firstly, this FCM method segments MR brain images, and then introduces an expert system to locate a landmark tissue by matching them with a prior model. Conventional FCM Pham et al has limitation of noise sensitivity and imperfection to the abnormality of brain *e.g.* tumor, edema, and cyst. Although k-means segmentation is noise immune, but it is prerequisite of this method that there should be perfect thresholding [21], which is quite hard for complex brain structure.

Furthermore, some research works describes only for tumor classification in [19], [22-24]. Due to having several limitations, aforesaid individual method cannot be used properly to detect tumor as well as its stages. Since it is foremost requirement of medical science is to detect tumor size and its stages, it is obligatory to segment proper tumor. As a result, there arises a demand of an optimum method which can be able to segment and detect actual tumor size, simultaneously.

1.3 Challenges

As the brain comprehends a complex structure for the computation and imaging so, there is some interesting notes which should be consider for the proposing any method for segmentation and classification. The presence of noise in MRI image cause blurring in the acquired results of segmentation. The proper segmentation of brain tumor presents hilarious results for the inhomogeneity of brain MRI image. There are some research works in [10-22] used techniques like region growing, thresholding, classifiers, Artificial Neural Networking (ANN), and clustering for segmentation. Based on these aforementioned techniques we can detect only brain tumor. For the classification of the brain tumor in MRI image it should be able to find the characteristics parameters so precisely as if it provides all the information about the nature of the tumor. From this values on can take decision or automatically processed the tumor category and stages.

Furthermore, some works describes only for tumor classification in [12-15]. There is a short of these techniques that they do not segment and classify the tumor and stages simultaneously. Due to having several limitations, aforesaid individual method cannot be used properly to detect tumor as well as its stages. Since it is foremost requirement of medical science is to detect tumor size and its stage, it is obligatory to segment proper tumor.

On the basis of these considerations, it is a challenge to propose a new style of segmentation and classification scheme for brain tumor that can be able to optimize the tumor with proper detection and classification for aforementioned conventional schemes. A general form of these two considerations is necessary to explain in the aspect of mathematical modeling. Else, the scheme would be able to implement itself in special purposes scheme.

1.4 Contribution of This Research

In this paper, basic segmentation schemes for brain tumour are analysed and their limitations are identified. Thereafter the concept to overcome the limitations is discussed. Consequently, a new style of Tumour detection in brain MRI image is presented that is called Template based K-means and modified Fuzzy C-means clustering (TKFCM) [77] and Linearized TKFCM [78] scheme to reach the stated challenges. By this idea, an algorithm is proposed which is used to detect the tumour position on the basis of the feature values of the given image and tumour. As the clustering algorithm is established from the measurement of the Euclidian distance from cluster centroid to the cluster points, so our algorithm is proposed that distances which depends on the feature values.

Unlike conventional k-means [21] and fuzzy c-means [32] in this scheme only the distances is allocated for the feature values like- contrast, energy, entropy, homogeneity, dissimilarity. The morphological operation along with enhancement of the image is required for the feature extraction. The template of the k-means algorithm is selected on the basis of temper of the brain tumour image. The modified fuzzy c-means algorithm based membership function is updated on the basis of the extracted feature of any tumour image. The decision whether there is any tumour or not, what are their condition, how would it affect to our brain is automatically provided and sometimes it required some experts. The measured values of the characteristics parameters such as area, eccentricity, bonding box, perimeter and orientation of the tumour and it stages are classified through the linearization and region properties algorithm of TKFCM.

Else these schemes are able to cope itself for special purpose use like tumour detection, drug designing, precautionary of tumour, tumour classification and automatic image processing etc. This factor can be varied according to the mathematical model of the proposed method to get the desired performances.

Beside this, the related algorithm of basic segmentation and classification schemes is discussed briefly. The performances of the proposed scheme are analysed in neural network as well as the other renowned classification scheme are also scrutinized by the numerically. By these results, the performances of the proposed scheme are compared with the existing conventional brain tumour detection and classification schemes graphically and elucidated the benefits as well as limitations of the proposed scheme.

1.5 Outlines of Thesis

- **Chapter 2** contains the Brain tumour overview and usual Magnetic Resonance Imaging techniques
- **Chapter 3** comprehends the brief discussion about the segmentation, its types and nature, difference of their quality and application.
- **Chapter 4** presents brain tumour detection and classification related works and their limitations.
- **Chapter 5** consists of the proposed Template based k-means and fuzzy c-means clustering (TKFCM) scheme for tumour detection. Performance of this method is performed through neural network.
- **Chapter 6** comprises with the linearization of TKFCM for tumour and its stages classification on the basis of some characteristics parameters.
- **Chapter 7** concludes the total work with clear explanation of applicability, benefits, and limitations of the proposed schemes. The scope of future work is also analysed in this section.

CHAPTER 2

Brain Tumor and Magnetic Resonance Imaging

Chapter Outlines

- ❖ Introduction
- ❖ Brain Anatomy Overview
- ❖ Types of Brain Tumour
- ❖ Magnetic Resonance Imaging
- ❖ MRI and Characteristics of Brain Tumour
- ❖ Difficulties in Segmentation in Brain MRI
- ❖ Summary

Brain Tumor and Magnetic Resonance Imaging

2.1 Introduction

Brain is the part of control system of our body. Nobody can be able to conscious if they do not have enough knowledge about the brain tumor which can affect them. This tumor causes a hilarious damage to the whole body, so symptoms and types of tumors need to be known. Again, the imaging techniques which is widely recognized and gold accepted also to be learnt. Magnetic Resonance Imaging (MRI) is one of the imaging processes that are used for the brain imaging. So, this widely accepted MRI is also discussed along with brain tumor in this chapter.

2.2 Brain Anatomy Overview

The human brain which functions as the center for the control of all the parts of human body is a highly specialized organ that allows a human being to adapt and endure varying environmental conditions. The human brain enables a human to articulate words, execute actions, and share thoughts and feelings. In this section the tissue structure and anatomical parts of the brain are described to understand the purpose of this study. The brain is composed of two tissue types, namely gray matter (GM) and white matter (WM). Gray matter is made of neuronal and glial cells, also known as neuroglia or glia that controls brain activity and the basal nuclei which are the gray matter nuclei located deep within the white matter. The basal nuclei include: caudate nucleus, putamen, pallidum and claustrum. White matter fibers consist of many delineated axons which connect the cerebral cortex with other brain regions. The left and the right hemispheres of the brain are connected by corpus callosum which is a thick band of white matter fibers. The brain also contains cerebrospinal fluid (CSF) which consists of glucose, salts, enzymes, and white blood cells. This fluid circulates through channels (ventricles) around the brain and the spinal cord to protect them from injury. There is also another tissue called meninges which are the membrane covering the brain and spinal cord [25].

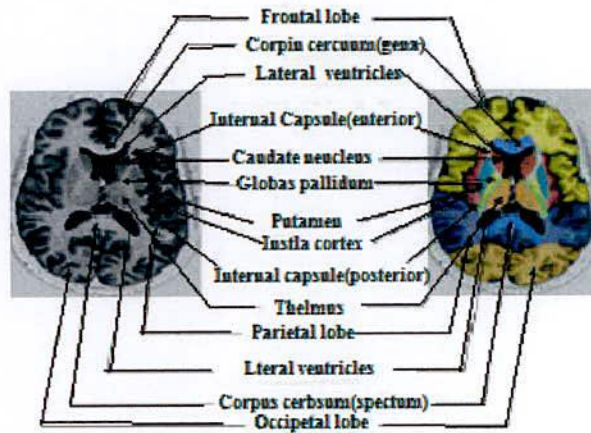


Figure 2.1: Overview Structure of Human Brain, Left Side: An Axial Slice MR Image, Right Side: the Color Coded Version of Image Left Side [26]

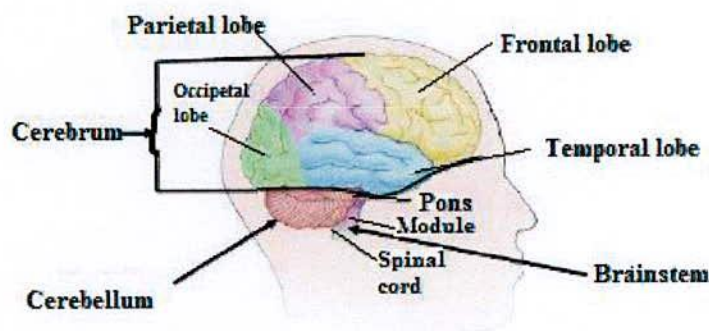


Figure 2.2: The Major Subdivision of Human Brain [26]

Figure 2.1 and Figure 2.2 show the anatomy of the brain. It is composed of the cerebrum and the brain stem. The cerebrum occupies the largest part of the brain. It is connected with the conscious thoughts, movement and sensations. It further consists of two halves, the right and the left hemispheres. Each controls the opposite side of the body. Moreover, each hemisphere is divided into four lobes: the frontal, temporal, parietal and occipital lobes. The cerebellum is the second largest structure of brain. It is connected with controlling motor functions of body such as walking, balance, posture and the general motor coordination. It is situated toward the back side of the brain and is linked to brain stems. Both, cerebellum and cerebrum have a very thin outer cortex of gray matter, internal white matter and small but deeply situated masses of the gray matter. The spinal cord is connected to the brainstem. It is located toward the bottom of the

brain. Brainstem controls vital functions in human body such as motor, sensory pathways, cardiac, repository and reflexes. It has three structures: the midbrain, pons and medulla oblongata [25].

2.3 Brain Tumors

Living creatures are made up of cells. The adult body normally forms new cells only when they are needed to replace old or damaged ones. Infants and children create new cells to complete their development in addition to those needed for repair. A tumor develops if normal or abnormal cells multiply when they are not needed [27].

A brain tumor is a mass of unnecessary cells growing in the brain or central spine canal. Brain tumors are a heterogeneous group of central nervous system neoplasms that arise within or adjacent to the brain. Moreover, the location of the tumor within the brain has a profound effect on the patient's symptoms, surgical therapeutic options, and the likelihood of obtaining a definitive diagnosis. The location of the tumor in the brain also markedly alters the risk of neurological toxicities that alter the patient's quality of life [28].

Every year there is number of brain tumor affected people of different ages which are increasing. The statistics shows profound results which describe how much the central nervous system (CNS) are under threat with the step of their age. There is a Figure 2.3 which is based on some data statistics.

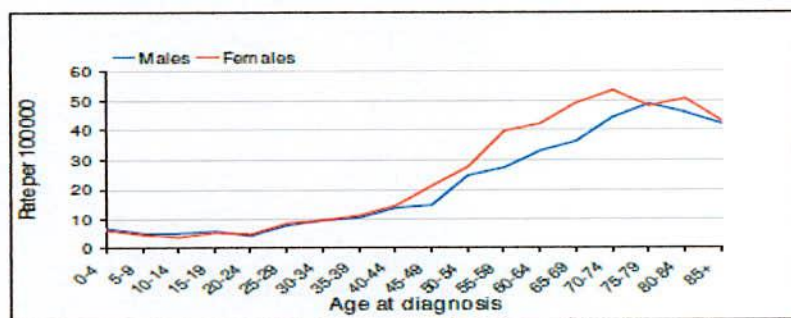


Figure 2.3: Age-specific incidence rates of tumors within CNS, meninges, cranial nerves and peripheral nervous system, 2000-2004, Norway. Malignant and benign [Source: Cancer Registry of Norway, 2004]

2.4 Types of Brain Tumors

Scientists have classified brain tumor according to the location of the tumor, type of tissue involved, whether they are noncancerous or cancerous. The site of the origin (primary or secondary) and other factors involved [29]. World Health Organization (WHO) classified brain tumor into 120 types. This classification is done on the basis of the cell origin and the behavior of the cell from less aggressive to more aggressive behavior. Even, some tumor types are graded ranging from grade I (less malignant) to grade IV (more malignant). This signifies the rate of the growth despite of variations in grading systems which depends on the type of the tumor [30].

There are two basic kinds of brain tumors– primary brain tumors and metastatic brain tumors. Primary brain tumors start and tend to stay, in the brain. Metastatic brain tumors begin as cancer elsewhere in the body and spread to the brain [27].

2.4.1 Primary Brain Tumors

A tumor that starts in the brain is a primary brain tumor. Glioblastoma multiform, astrocytoma, medulloblastoma and ependymoma are examples of primary brain tumors. Primary brain tumors are grouped into benign tumors and malignant tumors [31].

2.4.1.1 Benign Brain Tumors

A benign brain tumor consists of very slow-growing cells, usually has distinct borders and rarely spreads. When viewed under a microscope, these cells have an almost normal appearance. Surgery alone might be an effective treatment for this type of tumor. A brain tumor composed of benign cells, but located in a vital area, can be considered life-threatening – although the tumor and its cells would not be classified as malignant [28].

2.4.1.2 Malignant Brain Tumors

A malignant brain tumor is usually rapid-growing, invasive and life-threatening. Malignant brain tumors are sometimes called brain cancer. However, since primary brain tumors rarely spread outside the brain and spinal cord, they do not exactly fit the general definition of cancer [28].

Malignant brain tumors that are cancerous can spread within the brain and spine. They rarely spread to other parts of the body. They lack distinct borders due to their tendency to send “roots”

into nearby normal tissue. They can also shed cells that travel to distant parts of the brain and spine by way of the cerebrospinal fluid. Some malignant tumors, however, do remain localized to a region of the brain or spinal cord [27]. Furthermore, Malignant tumor can be classified in some stages like- i) tissue area is like normal tumor which just congested in an area is stage I, ii) tumor with or without lymph node but not enough spreading is referred as stage II, iii) stage III-tumor fixed or spread enough above collarbone, and iv) stage IV is known as tumors which spread to other parts (metastasis) of body [4].

2.4.2 Metastatic Brain Tumors

Cancer cells that begin growing elsewhere in the body and then travel to the brain form metastatic brain tumors. For example, cancers of the lung, breast, colon and skin (melanoma) frequently spread to the brain via the bloodstream or a magnetic-like attraction to other organs of the body. All metastatic brain tumors are, by definition, malignant and can truly be called “brain cancer” [31].

2.5 Magnetic Resonance Imaging (MRI)

Raymond V. Damadian invented MRI in 1969 and was the first person to use MRI to investigate the human body [33]. Eventually, MRI became the most preferred imaging technique in radiology because MRI enabled internal structures be visualized in some detail. With MRI, good contrast between different soft tissues of the body can be observed. This makes MRI suitable for providing better quality images for the brain, the muscles, the heart and cancerous tissues compared with other medical imaging techniques, such as computed Tomography (CT) or X-rays [34]. In MRI signal processing considers signal emissions. These are characterized by various magnetic signals weighting with particular values of the echo time (T_g) and the repetition time (T_r). The signal processing has three different images that can be achieved from the same body: T1-weighted, T2-weighted and PD-weighted (proton density).

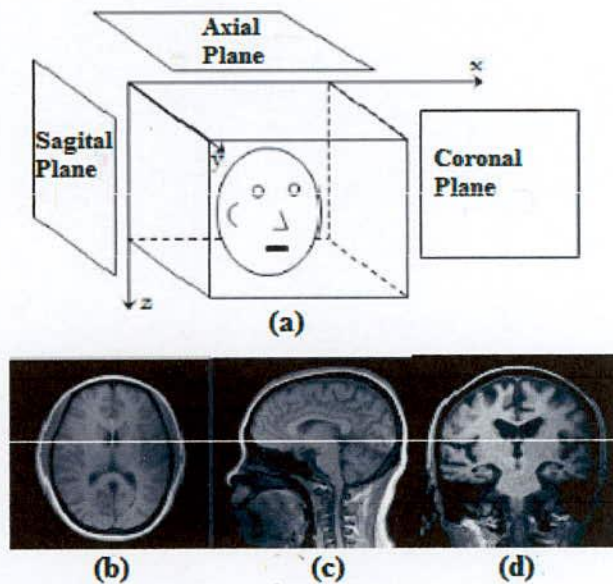


Figure 2.4: (a) Brain MR images form, (b) axial plane, (c) sagittal plane and (d) coronal plane [26].

Figure 2.4 (a) shows that a patient's head is examined from three plans in a clinical diagnosis which are plane, sagittal plane and coronal plane. Furthermore, T1-weighted brain MR images from various planes are shown in Figure 2.4 (b), (c), and (d).

There are two main MR imaging sequence families, depending on the type of echo recorded: spin echo sequence and gradient echo sequences. Spin echo (SE) sequence with its variant fast spin echo (FSE) sequence has been the standard MRI pulse sequences for anatomical and pathological details [35]. Brain images in MRI scan can be normal or abnormal. The normal brain is characterized by having gray matter (GM), white matter (WM) and cerebrospinal fluid (CSF) tissues. The abnormal brain usually contains active tumor, necrosis and edema in addition to normal brain tissues. Necrosis is a dead cell located inside an active tumor, while edema is located near active tumor borders. Edemas, which results from local disruption of blood brain barrier, often overlap with normal tissues and it is always difficult to distinguish from the other tissues [36].

An image from MRI scan is composed of gray level intensity values in the pixel spaces. The gray level intensity values depend on the cell concentration in the volume scanned. A darker region indicates the presence of some abnormality.

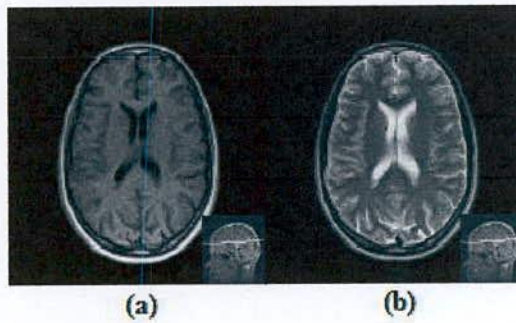


Figure 2.5: Original raw MRI data from Pioneer Diagnostic Center (a) T1-w axial scan image, (b) T2-w axial scan image [26].

In normal brain MR images, image intensity level for brain tissues is of the order of increasing brightness from CSF, GM to WM in T1-weighted (T1-w) and from WM, GM to CSF in T2 weighted (T2-w) image. This is illustrated in Figure 2.5.

In tumorous brain, MR images intensity level of tumorous tissues exhibit different intensity level on T1-w and T2-w images based on the type of tumor. On T1-w, most tumors have low or intermediate signal intensity but for some tumors this does not hold true, for example, glioblastoma multiform tumor has high signal intensity. On T2-w most tumors have bright intensity but there are tumors which have low intensity, the classic examples are lymphoma tumors [36]. Figure 2.6 shows some example of tumors intensity level characteristics in MRI.

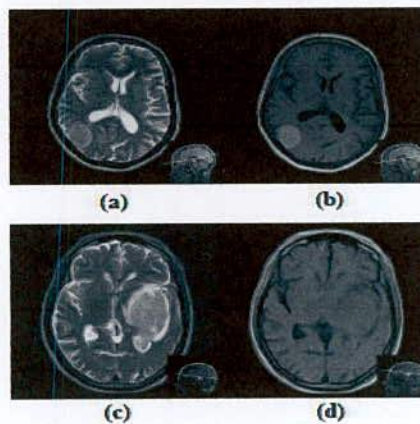


Figure 2.6: Tumor region intensity characteristics, original raw MRI data from Pioneer Diagnostic Center. (a) and (c) T2-w images, (b) and (d) T1-w Images. Tumor region in (a) Low Intensity, (b) High Intensity, (c) High Intensity and (d) Low Intensity [26]

2.6 MRI Brain Imaging and Characteristics of Brain Tumors

There are a variety of imaging techniques used to study brain tumors, such as: magnetic resonance imaging (MRI), computed tomography (CT), positron emission tomography (PET), and single photon emission computer tomography (SPECT) imaging and cerebral angiography. In recent years, CT and MR imaging are the most widely used techniques, because of their widespread availability and their ability to produce high resolution images of normal anatomic structures and pathological tissues. Magnetic resonance imaging (MRI) is a method used to visualize pathological or other physiological alterations of living tissues and is commonly used for brain tumor imaging because of the following reasons [37]. It does not use ionizing radiation like CT, SPECT and PET. Its contrast resolution is higher than other techniques mentioned above ability of MRI devices to generate 3D space images enables them to have superior tumor localization its ability in acquisition of both functional and anatomical information about the tumor during the same scan. Before discussing the MR image characteristics of brain tumors, it is important to describe the working principle of MR imaging. During MR imaging, the patient is placed in a strong magnetic field which causes the protons in the water molecule of the body to align in either a parallel (low energy) or anti-parallel (high energy) orientation with the magnetic field. Then a radiofrequency pulse is introduced which forces the spinning protons to move out of equilibrium state. When a radio frequency pulse is stopped, the protons return to equilibrium state and produce a sinusoidal signal at a frequency dependent on the local magnetic field.

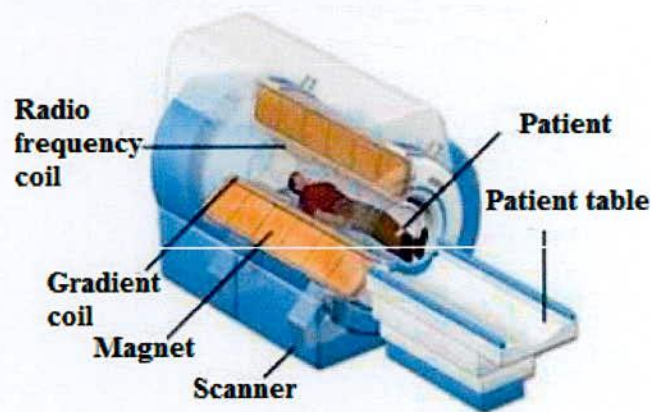


Figure 2.7: MRI scanner cutaways [26].

Finally, a radio frequency coils or resonators within the scanner detects the signal and creates the image [38]. Magnetic-resonance imaging (MRI) is an imaging technique used primarily in medical settings to produce high quality images of the inside of the human body. A MRI is similar to CT, but it does not use X-rays. Instead, a strong, magnetic field is used to affect the orientation of protons, which behave like miniature magnets and tend to align themselves with the external field.

2.7 Difficulties in Segmentation of Brain MRI

Cortical segmentation has not been made fully automated and operated at high speed because of the reliability of the MRI with regards to the homogeneity of its magnetic field. The problems of MRI include:

Noise: Random noise connected with MR imaging system. This is known to have a Rician distribution [39].

Intensity Inhomogeneity also called Bias Field or Shading Artifact: The non-uniformity in the radiofrequency (RF) field during data collection results in shading effect [40].

Partial Volume Effect: In this type of effect more than one type of class or tissue occupies one pixel or voxel of an image. The pixels or voxels are called mixels [41].

Segmentation of MRI outputs are normally done by medical experts and requires processes which consume time. As the images of tumor tissues from different patients contain many diverse appearance and gray level intensities and frequently look similar to normal tissues, the process of automation for segmentation of MRI outputs faces many challenges. One of these challenges is overcome by utilizing prior information about the appearance of normal brain when performing classification from a multi-dimensional volumetric features set. This is tantamount to using a statistical model for tumor and normal tissue of the same feature set. Manual segmentation and analysis of MR brain tumor images by radiologists is carried out in nearly all Hospitals at the present moment. The reliability of the segmentation depends on the knowledge and skill of the radiologists. However, the process is manual, tedious, time-consuming, highly subjective and impractical in today's medical imaging diagnosis where large numbers of images are taken for a single patient. As a result, there is strong demand to automate the tumor detection and segmentation process. Even though, there are numerous efforts and promising results in medical imaging community. There are still some challenges such as accurate and reproducible segmentation and characterization of abnormalities using

medical imaging community. There are still some challenges such as accurate and reproducible segmentation and characterization of abnormalities using intelligent algorithms due to the variety of shapes, locations and image intensities of different brain tumors. This thesis paper in which a new TKFCM method is proposed focuses on developing an automated brain tumor detection and segmentation system. This will enhance the detection and visualization of brain tumors from the output of MRI scans.

2.8 Summary

This chapter is discussed about the basics of brain and brain tumor along with gold accepted conventional Magnetic Resonance Imaging (MRI) technique. This discussion can be summarized as below:

- ✓ The basic brain anatomy is overviewed for the usual researchers.
- ✓ Different types of tumor and their stages are mentioned very precisely which will be helpful for further research.
- ✓ The MRI technique, its operation for the brain and their imaging process are discussed consequently.
- ✓ Difficulties in segmentation is presented in this chapter for the betterment of the further research in this field

CHAPTER 3

Segmentation of Brain MRI Image

Chapter Outlines

- ❖ Introduction
- ❖ Image Segmentation
- ❖ Summary

Segmentation of Brain MRI Image

3.1 Introduction

Diagnostic imaging is an invaluable tool in medicine today. Magnetic resonance imaging (MRI), computed tomography (CT), digital mammography, and other imaging modalities provide an effective means for noninvasively mapping the anatomy of a subject. These technologies have greatly increased knowledge of normal and diseased anatomy for medical research and are a critical component in diagnosis and treatment planning. With the increasing size and number of medical images, the use of computers in facilitating their processing and analysis has become necessary. In particular, computer algorithms for the delineation of anatomical structures and other regions of interest area key component in assisting and automating specific radiological tasks. These algorithms, called *image segmentation* algorithms, play a vital role in numerous biomedical imaging applications such as the quantification of tissue volumes [42], diagnosis [43], localization of pathology [70], study of anatomical structure [44], treatment planning [45], partial volume correction of functional imaging data [46], and computer integrated surgery [47, 48]. Here in this following section we will collaborate a brief about the segmentation.

3.2 Image Segmentation

The purpose of segmentation is to separate an image information into clear meaningful parts by placing boundaries separating the area of the healthy brain from the area of the cancerous and tumorous brain. Segmentation must not allow regions of the image to overlap. Segmentation can be therefore formally defined as follows:

If F is the set of all pixels and $P()$ is a homogeneity predicate defined on groups of connected pixels, then segmentation is a partitioning of the set F into a set of connected subsets or regions (S_1, S_2, \dots, S_n) such that:

$$\bigcup_{i=1}^n S_i = F \tag{1}$$

With,

$$S_i \cap S_j = \emptyset \quad \text{and} \quad i \neq j \tag{2}$$

Homogeneity predicates, $P()$ are usually based on image intensity, color, texture, etc.

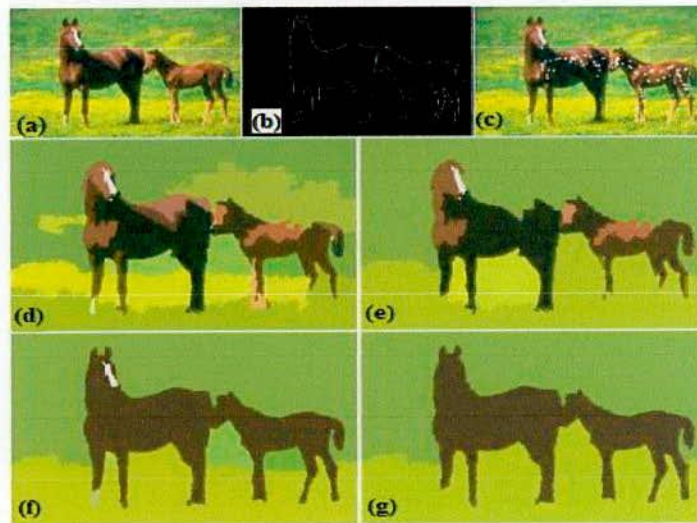


Figure 3.1: Basic segmentation with different criteria. (a) Original image. (b) Ground truth-based border image. (c) Seeded image. (d) and (e) Segmentation results using the RGB as color space presenting their best rand index and best BGM, respectively. (f) and (g) Segmentation results using the adaptive discrimination function generated by the seed points in (c) presenting, respectively, the results with best rand index and best BGM index [13].

A great variety of segmentation methods has been proposed in the past decades for brain MRI image, and some categorization is necessary to present the methods properly here. A disjunctive categorization does not seem to be possible though, because even two very different segmentation approaches may share properties that defy singular categorization¹. The categorization presented in this chapter is therefore rather a categorization regarding the *emphasis* of an approach than a strict division [27].

The following categories are used for the segmentation of brain MRI image:

3.2.1 Threshold based segmentation

Histogram thresholding and slicing techniques are used to segment the image. They may be applied directly to an image, but can also be combined with pre- and post-processing techniques. When several desired segments in an image can be distinguished by their grey values, threshold segmentation can be extended to use multiple thresholds to segment an image into more than two segments [13]: all pixels with a value smaller than the first threshold are assigned to segment 0,

assigned to segment 1, all pixels with values between the second and third threshold are assigned to segment 2, etc. If n thresholds (t_1, t_2, \dots, t_n) are used:

$$g(v) = \begin{cases} 0 & \text{if } v < t_1 \\ 1 & \text{if } t_1 \leq v < t_2 \\ 2 & \text{if } t_2 \leq v < t_3 \\ \vdots & \vdots \\ n & \text{if } t_n \leq v \end{cases} \quad (3)$$

After thresholding, the image has been segmented into $n+1$ segments identified by the gray values 0 to n respectively. Figure 3.2 shows an example using two thresholds.

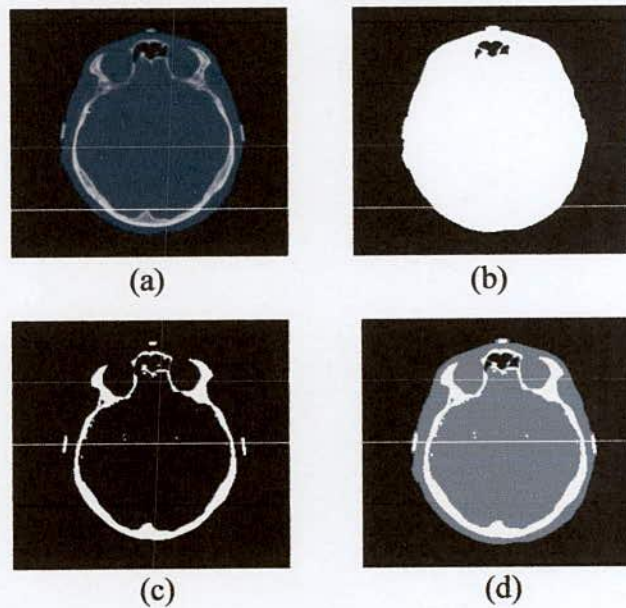


Figure 3.2: Example of using multiple thresholds for segmentation. (a) original image (b) thresholding result after using a low threshold value to segment the image into head and background pixels (c) result after using a higher value to segment the bone pixels (d) result after using both thresholds at once [26].

3.2.2 Edge based segmentation

With this technique, detected edges in an image are assumed to represent object boundaries, and used to identify these objects. Since a (binary) object is fully represented by its edges, the segmentation of an image into separate objects can be achieved by finding the edges of those objects. A typical approach to segmentation using edges is (1) compute an edge image, containing all(plausible) edges of an original image, (2) process the edge image so that only closed object boundaries remain, and (3) transform the result to an ordinary segmented image by filling in the object boundaries. The edge detection step (1) has been discussed. The third step, the filling of boundaries, is not a difficult step, and an example of how this can be achieved is given for the technique below. The difficulty often lies in the middle step: transforming an edge (or edginess) image to closed boundaries often requires the removal of edges that are caused by noise or other artifacts, the bridging of gaps at locations where no edge was detected (but there should logically be one) and intelligent decisions to connect those edge parts that make up a single object. The section on edge linking below addresses some of these difficulties. The next sections on watershed segmentation and active contours deal with methods that avoid having to link edge parts by manipulating like a rubber band— contours that are always closed until they best fit an edge image.

In the Figure 3.3, Top left: original 400×350 artificial image with added noise. Top middle: edginess image; computed using a scale space operator (f_w) with $\sigma = 1$ pixel. Top right: same image after thresholding. Bottom left: sign of Laplacian image. Laplacian image computed using a scale space operator (f_{ii}) with $\sigma = 1$ pixel. Bottom middle: product of Laplacian sign and thresholded edge image. Bottom right: result after filling in of the boundaries as in the algorithm above. The noise was added to the original image to show some of the artifacts that they cause: notches in the edges of segmented objects, and lines where the filling algorithm encounters erroneous sign transitions. If no or less noise is added to the original, the segmentation result is perfect.

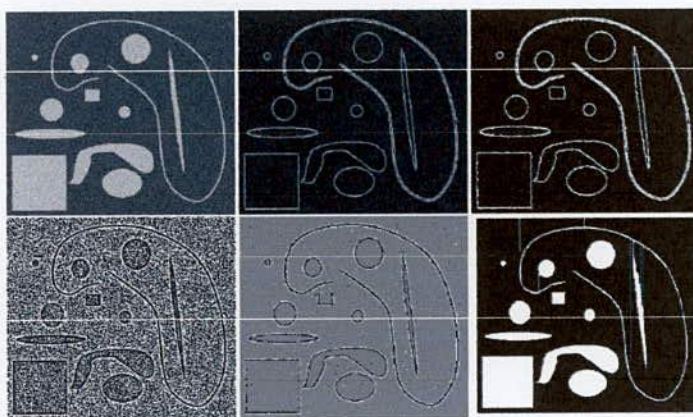


Figure 3.3: Example of edge-based segmentation [13].

3.2.3 Region Based Segmentation

Where an edge based technique may attempt to find the object boundaries and then locate the object itself by filling them in, a region based technique takes the opposite approach, by (*e.g.*) starting in the middle of an object and then “growing” outward until it meets the object boundaries. In the previous section, objects were found by locating their boundaries. In this section, we discuss the dual approach of finding the object *region* instead of its edges. In theory, finding an object by locating its boundary and finding it by establishing the region it covers will give you exactly the same object; the boundary and the region are just different representations of the same object. In practice, however, taking an edge based approach to segmentation may give radically different results than taking a region based approach. The reason for this is that we are bound to using imperfect images and imperfect methods; hence the practical result of locating an object boundary may be different from locating its region [13].

Many merging methods of segmentation use a method called *region growing* to merge adjacent single pixel segments into one segment. Region growing needs a set of starting pixels called *seeds*. The region growing process consists of picking a seed from the set, investigating all 4 connected neighbors of this seed, and merging suitable neighbors to the seed. The seed is then removed from the seed set, and all merged neighbors are added to the seed set. The region growing process continues until the seed set is empty. An example of this segmentation is shown in Figure 3.4.

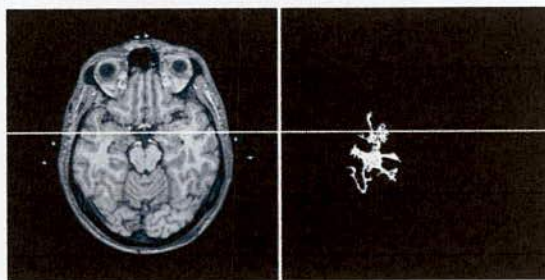


Figure 3.4: Example of region growing based on a gray level range. On the left, an original 256×256 image is shown, with a gray level range of 256. On the right, the result of region growing with the seed roughly at the center of the structure, allowing a gray value range of ± 30 around the gray value of the seed [13].

3.2.4 Clustering Techniques

Although clustering is sometimes used as a synonym for (agglomerative) segmentation techniques, we use it here to denote techniques that are primarily used in exploratory data analysis of high-dimensional measurement patterns. In this context, clustering methods attempt to group together patterns that are similar in some sense. This goal is very similar to what we are attempting to do when we segment an image, and indeed some clustering techniques can readily be applied for image segmentation.

Clustering techniques is the collective name for methods that attempt to group together measurements points ('patterns'). For an off-topic example in [13], let's say we measure the weight and length of a population of rabbits. We can then plot the measurements of each rabbit together as shown in Figure 3.5. When looking at the figure, it will be clear that three clusters can be identified—there are very likely three types of rabbit in the population. The object of clustering techniques is to identify such clusters in data. The relation to segmentation will be clear; when viewing the rabbit plot as an image, the most intuitive segmentation would be to divide the image into segments equal to the three clusters and the background.

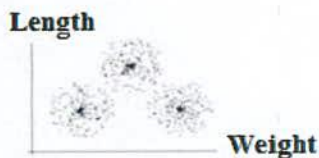


Figure 3.5: Finding clusters of measurement data points is often similar to image segmentation [13].

3.2.5 Matching

When we know what an object we wish to identify in an image (approximately) looks like, we can use this knowledge to locate the object in an image. This approach to segmentation is called matching.

If we want to locate an object in an image, and we have available an example of what it should look like (a *template*), we can find this object by matching the template to various image locations until we have found the object. For an example, see Figure 3.6. The most straightforward way of determining whether a template ‘fits’ would be to place the template at a certain image location, and see whether the grey values of the template and the underlying image image grey values all match. However, because there will generally be some differences between the image and template values because of noise and other artifacts, this is not a very practical method. More useful is a quantitative measure of fit such as [13]:

$$M_1(p, q) = \sum_{x=0}^{M-1} \sum_{y=0}^{N-1} (g(x, y) - f(x+p, y+q))^2 \quad (4)$$

where f is the image, g the $M \times N$ template, and the variables p and q determine the location of the template in the image, see Figure 3.7 This measure will be small if the template is similar to the part of the image under investigation; then all grey value differences $g(x, y) - f(x+p, y+q)$ are small and the sum M_1 will be small. The location of optimal template fit is found by minimizing M_1 to p and q .



Figure 3.6 Image matching based segmentation. The left image gives a template of the object which is wished to locate in the right image. This is achieved by matching of the template to various locations in the right image [26].

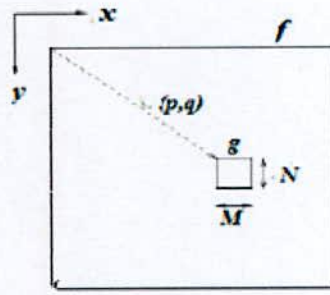


Figure 3.7: Definitions for image matching [13].

Besides the squared form M_1 , another often used measure is M_2 , which uses the actual gray value differences instead of their squares:

$$M_2(p, q) = \sum_{x=0}^{M-1} \sum_{y=0}^{N-1} |(g(x, y) - f(x+p, y+q))| \quad (5)$$

M_2 puts less weight on relatively large gray value differences than M_1 . But perhaps the most commonly used measure is the *cross correlation* M_3 , which is defined by

$$M_3(p, q) = \sum_{x=0}^{M-1} \sum_{y=0}^{N-1} |(g(x, y) f(x+p, y+q))| \quad (6)$$

The maximum of M_3 with respect to p and q is assumed to indicate the location in the image where the template fits best. There is a strong relation between the measures M_1 and M_3 , which is most obvious if the sums in the measure M_1 are extended to the entire image f (and pad the template g with zeros); then the measure M_3 appears literally between constants if we expand the square:

$$\begin{aligned} M_1^*(p, q) &= \sum_{x=0}^{M-1} \sum_{y=0}^{N-1} (g(x, y) - f(x+p, y+q))^2 \\ &= \sum \sum f^2(x, y) - 2 \sum \sum (g(x, y) f(x+p, y+q)) + \sum \sum g^2(x-p, y-q) \end{aligned} \quad (7)$$

where d_x and d_y are the dimensions of the image f .

According to Harlick and Shapiro et al, image segmentation can be classified into three categories: spatial clustering split and merge schemes, and region growing schemes.

3.2.6 Spatial clustering

Image segmentation and image clustering are different. In image segmentation, the grouping of the image is carried out in spatial domain. In image clustering, grouping is performed in the measurement space. Overlapping regions can be the result of clustering. It is not possible to produce overlapping regions from segmentation. Clustering and spatial segmentation can be combined to form spatial clustering, which combine histogram techniques with spatial linkage techniques for better results [13].

3.2.7 Split and merge segmentation

The split method begins with the entire image, and repeatedly splits each segment into quarters if the homogeneity criterion is not satisfied. These splits can sometimes divide portions of one object. The merge method joins adjacent segments of the same object [49]. It is important to distinguish the separate regions for intensity based segmentation so that over segmentation and under-segmentation of regions can be differentiated. Task of this kind can be performed using split segmentation or merge segmentation. If a region is not segmented fully, correction can be made by adding boundaries to, or splitting, certain regions that contain parts of different objects. If a region is segmented more than is necessary, correction can be made by eliminating false boundaries and merging adjacent regions if they belong to the same object or feature.

3.2.8 Region Growing

Region growing connects neighboring points to make bigger region. The process of region growing is dictated by certain condition associated with the selection of a threshold value [49-51]. Seeded region growing starts with one or more seed points and then grows within the region to form a larger region satisfying some homogeneity constraint. The homogeneity of a region can be dependent upon any characteristic of the region in the image: texture, color or average intensity.

3.3 Summary

In this chapter described the following matters which are effective in point of concerning of the segmentation.

- ✓ The basic of segmentation is presented in point of tumor detection and classification.
- ✓ The different kind of segmentation for different image criterion is also clarified with expressions.
- ✓ The relevant example of the each segmentation is presented in Figure 3.2 -3.7.

CHAPTER 4

Conventional Techniques for Brain Tumor Detection

Chapter Outlines

- ❖ Introduction
- ❖ Conventional Techniques for Brain Tumor Detection
- ❖ Summary

Conventional Techniques for Brain Tumor Detection

4.1 Introduction

The automated detection and segmentation of brain tumor from MR helps to overcome the time taking process of manual segmentation of large datasets, which is discussed in chapter 3. It also ensures reproducibility which is normally affected by inter and intra observer variability. However, automated systems are not without problems to achieve these objectives. For example, some of the major problems are pixel intensities violate the independent and identically distributed assumptions of images due to very nature of the brain MR images, presence of a considerable amount of artifacts and intensity inhomogeneity in MR images [52]-[53]. There is a need that automated method must consider these problems in order to achieve the reproducible segmentation results and to develop clinically accepted automated methods.

4.2 Conventional Techniques for Brain Tumor Detection

In recent years, many methods have been suggested for automation of scanning, imaging and identification of brain tumors. These methods can be classified into two: intelligent based and non-intelligent based method. Intelligent based method includes artificial neural networks, Fuzzy logic, support vector machine, and hybrid process. The non-intelligent based method includes thresholding, and region growing. However, there is no clear division between the two methods. Often, intelligent based method is used as non-intelligent. But it is modified to refine the output. In the following many notable methods have been briefly discussed.

4.2.1 Thresholding

In thresholding approach, image segmentation is based on gray level intensity value of pixels. A thresholding procedure attempts to determine an intensity value, called the threshold, which separates the desired classes. The segmentation is then achieved by grouping all pixels with intensity greater than the threshold into one class, and all other pixels into another class [54].

However, thresholding is often used as an initial step in a sequence of image segmentation process. Image segmentation through thresholding is considered to be a simple and powerful

approach to segment the images that have light objects on dark background [55]. Thresh holding is a technique which is based on image space region, that is, on characteristics of image [56]. It converts a multilevel image into a binary image. For example, it selects a proper thresh hold in order to divide image pixels into many regions and spate objects form the background. Any pixel (x, y) is deemed as part of the object, provided that its intensity is greater than or equal to the threshold value [57-58]. On the basis of thresholding value, there are two types of threshold values such as global and local thresholding [59]. The approach is called global thresholding when the T is fixed or constant. Otherwise, it is called local thresholding. If the background illumination is uneven, the global thresholding is likely to fail. In local thresholding, multiple thresholds are used to compensate the uneven illumination [60].

Generally, the threshold selection is done interactively. However, it is possible to derive automatic threshold algorithms [10]. This includes segmentation of an image based on thresholding of histogram features and gray level thresholding and perhaps the simplest technique. This is particularly suitable for an image with region or object of uniform brightness placed against a background of different gray level. A threshold can be applied to segment the object and background. Threshold is defined mathematically as shown below:

$$C(i, j) = \begin{cases} 255 & p(i, j) \geq T \\ 0 & p(i, j) \leq T \end{cases} \quad (8)$$

Where, $C(i, j)$ is the resulting pixel at co-ordinate (i, j) and $p(i, j)$ is the pixel of the input image and T is the threshold value. Equation (8) gives excellent results for segmentation of image. Thresholding operation, defined by equation-1 is very basic and simple, and works well only when the object and background have uniform brightness of distinct gray level values respectively. This threshold operation does not work well at segmentation of images with multiple objects each having distinct gray level value varying over a band of values. To overcome this limitation, band thresholding based multiple thresholding operation is applied:

$$C(i, j) = \begin{cases} 1 & \text{for } T_1 < p(i, j) \leq T_2 \\ 2 & \text{for } T_2 < p(i, j) \leq T_3 \\ k & \text{for } T_k < p(i, j) \leq T_{k+1} \\ 0 & \text{Otherwise} \end{cases} \quad (9)$$

Here, the k^{th} band corresponds to the object or region having pixel values in the range of T_k to T_{k+1} where, T_k is the lower limit of gray level and T_{k+1} is the upper limit of gray level band.

Its main limitation is that only two classes are generated and it does not work when confronted with structures that lack clear borders. Hence, it cannot be applied in multicultural images. Moreover, thresholding does not consider the spatial characteristics of an image because of this it is sensitive to noise [57]. Both these artifacts, thus, corrupt the histogram of the image making separation more complicated and difficult.

For application of thresholding based segmentation technique, it is required to apply the correct threshold values in order to achieve proper segmentation results, otherwise results are poor. The real time image example of segmenting image through thresholding can be shown in following Figure 4.1.

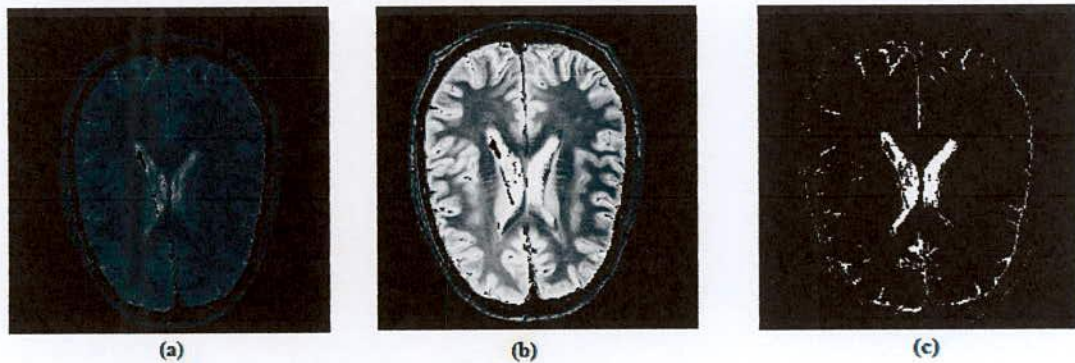


Figure 4.1 Thresholding based segmented brain MRI image. (a) Original spin density image (b) Enhanced image by histogram equalization (c) Segmented image (CSF tissue) 70 – 230. [Source: .ppt image segmentation region growing & contour following]

4.2.2 Region Growing

Region growing is a technique to extract a region of the image based on predefined criteria. In its simplest form, region growing requires a seed point that is manually selected by an operator, and extracts all pixels connected to the initial seed with the same intensity value. To eliminate the dependency on initial seeds and to make the method automatic statistical information and a prior knowledge can be incorporated in the algorithm. Region growing can be so sensitive to noise, that it may cause extracted regions to have holes or even is disconnected.

Conversely, overlapping gray value distribution in MR images can cause separate regions to become connected. Region growing is not often used alone because it is not sufficient to segment brain structures accurately and robustly. Pohle suggested that region growing can be an integrated technique using multilevel sets of boundary information [15]. In the algorithm, region growing is used as a propagation force and boundary information is used as a stopping criteria. Pohle successfully applied this technique to a total of 246 slices containing images of axial tumor obtained from 10 patients [15]. However, this method is semi-automatic as it relies on manual input seed region for region growing. A more accurate method needs precise anatomical information to locate initial seed pixels for each anatomical region and together with their associated homogeneity. Its reliability depends on accuracy of the model assumption non homogeneity and region characteristics.

As compared to edge detection method, segmentation algorithms based on region are simpler and have strongly immune to noise [56], [61]. Edge method divide an image based on frequent changes in intensity near the edges, while, region method divide an image into regions which are similar as per a set of predetermined criteria [55], [62].

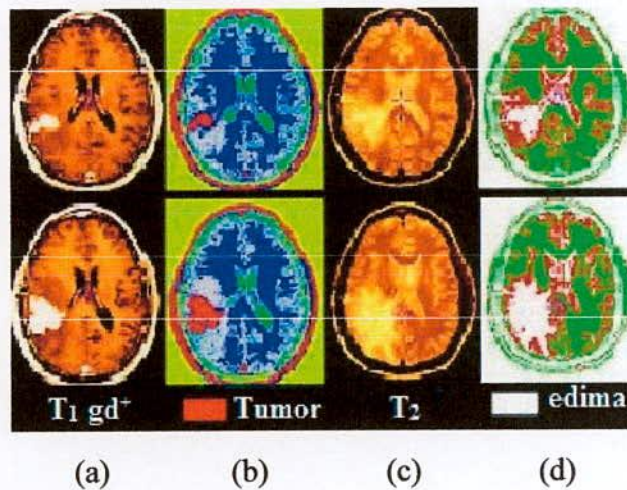


Figure 4.2: Region growing based segmentation (a) T_1 weighted brain MRI image (b) red marked tumor detection (c) T_2 weighted brain MRI image (d) white marked edema detection

Segmentation algorithms based on region consist of the following methods:

1. Region Growing: It is a procedure [58], [63] that puts pixels in a whole image together as a group into sub-regions or large regions based on the predetermined criterion [64]. Region growing processing consists of four steps:

- a. To select a group of seed pixels in an original image [65].
- b. To select a set of identical criterion like gray level intensity or color and develop a stopping rule.
- c. To grow regions by attaching to each seed the neighboring pixels that have predetermined properties similar to seed pixels.

2. Region Splitting and Merging: Instead of selecting a seed point, the users may divide an image into a set of arbitrary detached regions and merge the regions [56], [63] to satisfy the conditions for reasonable segmentation. Basically, region splitting or merging is implemented with a theory based on quad tree data. For example, let R represent the whole image region and choose a predicate Q .



Figure 4.3: Comparison of Region growing and Region split & Merge segmentation process

i. The method starts with the whole image if $Q(R) = false$ [63], and then it is demarcated the image into quadrants, if Q is false for any of the quadrant if $Q(R_i) = false$, thus, it is sub demarcated the quadrant into sub-quadrants and continue until no further splitting is possible.

ii. The final demarcation may have neighboring regions with identical properties, if only splitting is used. This weakness can be treated or by allowing both merging and splitting, that is, merging any neighboring region R_i & R_k for which, $Q(R_i \cup R_k) = true$.

iii. Stop where there is need for further merging.

The main limitations of this technique are like-

- Vulnerable to noise
- Difficult to find lines in complicated images
- Difficult to change the shape which looking for
 - Line : $y = ax + b$
 - Circle : $(x-C_1)^2 + (y-C_2)^2 = C_3 \rightarrow$ Three Dimensional parameter space
- Long processing time \rightarrow About 25 minutes for 192×128 size image by Pentium 166MHz, 48Mbyte RAM

4.2.3 Classifiers

Classifier methods are pattern recognition techniques that seek to partition a feature space derived from the image using data with known labels [66], [67]. A *feature space* is the range space of any function of the image, with the most common feature space being the image intensities themselves. A classifier based segmented image is shown in Figure 4.4 where, the edema and tumor is classified on the basis of the feature space. All pixels with their associated features on the left side of the partition would be grouped into one class. Although the features used can be related to texture or other properties, we assume for simplicity that the features are simply intensity values.

Classifiers are known as *supervised* methods since they require training data that are manually segmented and then used as references for automatically segmenting new data. There are a number of ways in which training data can be applied in classifier methods. A simple classifier is the nearest-neighbor classifier, where each pixel or voxel is classified in the same class as the training datum with the closest intensity. The k-nearest-neighbor (KNN) classifier is a generalization of this approach, where the pixel is classified according to the majority vote of the k closest training data. The KNN classifier is considered a nonparametric classifier since it makes no underlying assumption about the statistical structure of the data. Another nonparametric classifier is the Parzen window, where the classification is made according to the majority vote within a predefined window of the feature space centered at the unlabeled pixel intensity.

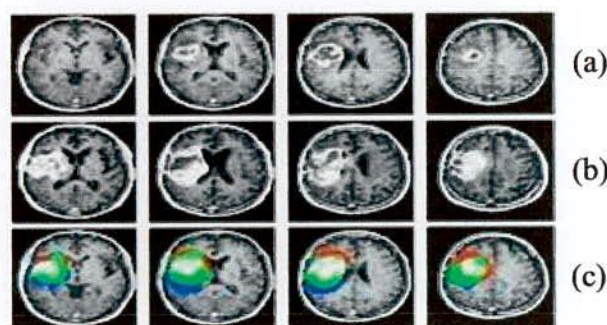


Figure 4.4: Classifier based segmented image. (a) Brain MRI image with edema (b) Brain MRI image with tumor (c) Brain MRI image with edema & tumor marked with different color.

A commonly-used parametric classifier is the maximum likelihood (ML) or Bayes classifier. It assumes that the pixel intensities are independent samples from a mixture of probability distributions, usually Gaussian. This mixture, called a finite mixture model, is given by the probability density function

$$f(y_j; \theta; \pi) = \sum_{k=1}^K \pi_k f_k(y_j; \theta_k) \quad (10)$$

Where, y_j is the intensity of pixel j , f_k is a component probability density function parameterized by θ_k , and $\theta = [\theta_1, \dots, \theta_k]$. The variables π_k are mixing coefficients that weight the contribution of each density function and $\pi = [\pi_1, \dots, \pi_k]$. Training data is collected by obtaining representative samples from each component of the mixture model and then estimating each θ_k accordingly. For Gaussian mixtures, this means estimating K means, covariance, and mixing coefficients. Classification of new data is obtained by assigning each pixel to the class with the highest posterior probability. When the data truly follows a finite Gaussian mixture distribution, the ML classifier can perform well and is capable of providing a soft segmentation composed of the posterior probabilities. Additional parametric and nonparametric classifiers are described in [68].

A disadvantage of classifiers is that they generally do not perform any spatial modeling. This weakness has been addressed in recent work extending classifier methods to segmenting images that are corrupted by intensity inhomogeneity [17]. Neighborhood and geometric information were also incorporated into a classifier approach in [69]. Another disadvantage is the requirement of manual interaction for obtaining training data. Training sets can be acquired for each image that requires segmenting, but this can be time consuming and laborious. On the other hand, use of the same training set for a large number of scans can lead to biased results which do not take into account anatomical and physiological variability between different subjects.

4.2.4 Artificial Neural Network

Artificial neural networks (ANNs) are massively parallel networks of processing elements or nodes that simulate biological learning. Each node in an ANN is capable of performing elementary computations. Learning is achieved through the adaptation of weights assigned to the connections between nodes. A thorough treatment on neural networks can be found in [70], [71]. ANNs represent a paradigm for machine learning and can be used in a variety of ways for image segmentation. The most widely applied use in medical imaging is as a classifier [18], [72], where the weights are determined using training data, and the ANN is then used to segment new data. ANNs can also be used in an unsupervised fashion as a clustering method [66], [73], as well as for deformable models [17]. Because of the many interconnections used in a neural network, spatial information can easily be incorporated into its classification procedures. Although ANNs are inherently parallel, their processing is usually simulated on a standard serial computer, thus reducing this potential computational advantage. There is a processed example of ANN is shown in Figure 4.5.

Artificial neural network has some limitation in point of computational time and training data. The training data is needed to be very precise, otherwise there would be complex in computation and guide to misdirection of detection. The network should be design as simple as possible otherwise there will be requiring much time to execute the data.

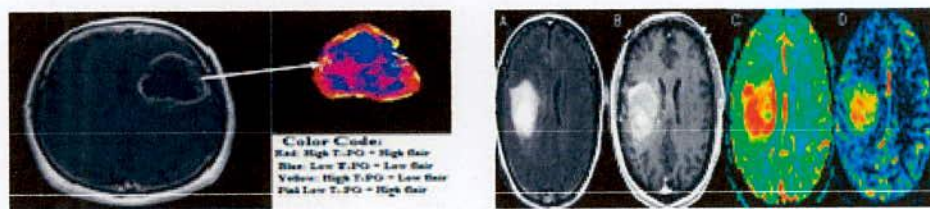


Figure 4.5: Color coded ANN based segmentation (left side) and example of ANN based brain MRI image segmentation (right side)

4.2.5 Expectation Maximization

The EM algorithm in [74-76] is an efficient iterative procedure to compute the Maximum Likelihood (ML) estimate in the presence of missing or hidden data. In ML estimation, we wish to estimate the model parameter(s) for which the observed data are the most likely. Each iteration of the EM algorithm consists of two processes: The E-step, and the M-step.

In the expectation, or E-step, the missing data are estimated given the observed data and current estimate of the model parameters. This is achieved using the conditional expectation, explaining the choice of terminology.

In the M-step, the likelihood function is maximized under the assumption that the missing data are known. The estimation of the missing data from the E-step is used in lieu of the actual missing data. Convergence is assured since the algorithm is guaranteed to increase the likelihood at each iteration.

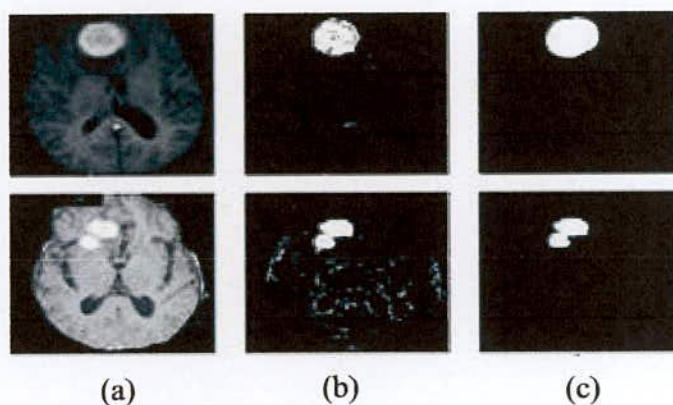


Figure 4.6: Expectation Maximization based segmented image. (a) Original image (b) E-stepped image (c) M-stepped image

4.2.6 Clustering

4.2.6.1 K-means Clustering

The conventional K-means of this section is discussed in [21]. Suppose, a data set $\{x_1, \dots, x_N\}$ consisting of N observations of a random D -dimensional Euclidean variable x . The goal of k-means is to partition the data set into some number K of clusters, where it should be supposed for the moment that the value of K is given. Intuitively, this might be thought of a cluster as comprising a group of data points whose inter-point distances are small compared with the distances to points outside of the cluster. It can be formalized this notion by first introducing a set of D -dimensional vectors c_k , where $k = 1, \dots, K$, in which c_k is a prototype associated with the k^{th} cluster. As it should be seen shortly, it can be thought of the c_k as representing the centers of the clusters. The goal is then to find an assignment of data points to clusters, as well as a set of vectors $\{c_k\}$, such that the sum of the squares of the distances of each data point to its closest vector c_k , is a minimum.

It is convenient at this point to define some notation to describe the assignment of data points to clusters. For each data point x_n , it has introduced a corresponding set of binary indicator variables $b_{nk} \in \{0, 1\}$, where, $k = 1, \dots, K$ describing which of the K clusters the data point x_n is assigned to, so that if data point x_n is assigned to cluster k then $b_{nk} = 1$, and $b_{nj} = 0$ for $j \neq k$. This is known as the 1-of- K coding scheme. In this method then define an objective function, sometimes called a distortion measure, given by [21]—

$$J = \sum_{n=1}^N \sum_{k=1}^K b_{nk} \|x_n - c_k\|^2 \quad (11)$$

Equation (11) represents the sum of the squares of the distances of each data point to its assigned vector c_k . The goal is to find values for the $\{b_{nk}\}$ and the $\{c_k\}$ so as to minimize J . It can be done this through an iterative procedure in which each iteration involves two successive steps corresponding to successive optimizations with respect to the b_{nk} and the c_k . First some initial values for the c_k are chosen. Then in the first phase J is minimized with respect to the b_{nk} , keeping the c_k fixed. In the second phase J is minimized with respect to the c_k , keeping b_{nk}

fixed. This two-stage optimization is then repeated until convergence. It would be seen that these two stages of updating b_{nk} and updating c_k correspond respectively to the E (expectation) and M (maximization) steps of the EM algorithm in [18], and to emphasize this and EM is used the terms E step and M step in the context of the K-means algorithm.

Consider first the determination of the b_{nk} . Because J in equation (11) is a linear function of b_{nk} , this optimization can be performed easily to give a closed form solution. The terms involving different n are independent and so it can be optimized for each n separately by choosing b_{nk} to be 1 for whichever value of k gives the minimum value of $\|x_n - c_k\|^2$.

In other words, it can be simply assigned the n^{th} data point to the closest cluster center. More formally, this can be expressed as [21]:

$$b_{nk} = \begin{cases} 1 & \text{if } k = \arg \min_a \|x_n - c_a\|^2, \quad a=1, \dots, k \\ 0 & \text{Otherwise} \end{cases} \quad (12)$$

Now consider the optimization of the c_k with the b_{nk} held fixed. The objective function J is a quadratic function of c_k , and it can be minimized by setting its derivative with respect to c_k to zero giving [21]

$$2 \sum_{n=1}^N b_{nk} (x_n - c_k) = 0 \quad (13)$$

in which this can easily solve for c_k

$$c_k = \frac{\sum_n b_{nk} x_n}{\sum_n b_{nk}} \quad (14)$$

The denominator in this expression is equal to the number of points assigned to cluster k , and so this result has a simple interpretation, namely set c_k equal to the mean of all of the data points x_n assigned to cluster k . For this reason, the procedure is known as the K -means algorithm.

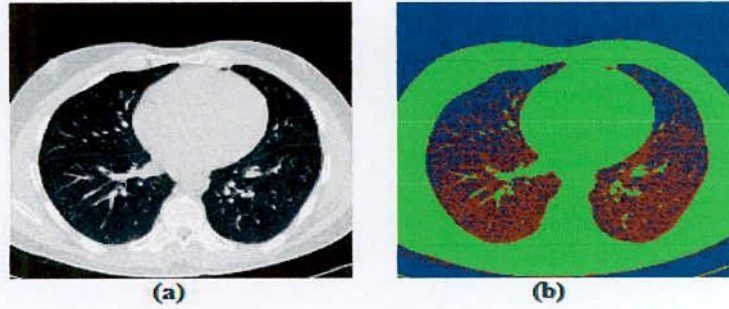


Figure 4.7: K-means clustering based image segmentation (a) Original image (b) Three-cluster image on gray values of image.

4.2.6.2 Fuzzy C-means Clustering

The fuzzy c-means (FCM) clustering algorithm, introduced by Bezdek, is an improvement of earlier clustering methods [32]. Let R be the set of real, R^P the set of p tuples of real, R^+ the set of nonnegative real, and W_{cn} the set of real $c \times n$ matrices. R^P will be called feature space, and elements $x \in R^P$ feature vectors; feature vector $x = (x_1, x_2, \dots, x_p)$ is composed of p real numbers.

Definition: Let X be a subset of R^P . Every function $u: X \rightarrow [0, 1]$ is said to assign to each $x \in X$ its grade of membership in the fuzzy set u . The function u is called a fuzzy subset of X . Note that there are infinitely many fuzzy sets associated with the set X . It is desired to "partition" X by means of fuzzy sets. This is accomplished by defining several fuzzy sets on X such that for each $x \in X$, the sum of the fuzzy memberships of x in the fuzzy subsets is one.

Definition: Given a finite set $X \subseteq R^P$, $X = \{x_1, x_2, \dots, x_n\}$ and an integer c , $2 \leq c \leq n$, a fuzzy c partition of X can be represented by a matrix $U \in W_{cn}$ whose entries satisfy the following conditions.

- 1) Row i of U , say $U_i = (u_{i1}, u_{i2}, \dots, u_{in})$ exhibits the i^{th} membership function (or i^{th} fuzzy subset) of X .
- 2) Column j of U , say $U_j = (u_{1j}, u_{2j}, \dots, u_{nj})$ exhibits the values of the c membership functions of the j^{th} data in X .

- 3) u_{ik} shall be interpreted as $u_i(x_k)$, the value of the membership function of the i^{th} fuzzy subset for the k^{th} data.
- 4) The sum of the membership values for each x_k is one (column sum $\sum_i u_{ik} = 1 \forall k$).
- 5) No fuzzy subset is empty (row sum $\sum_k u_{ik} > 0 \forall i$).
- 6) No fuzzy subset is all of X (row sum $\sum_k u_{ik} > n \forall i$).

M_{fc} will denote the set of fuzzy c partitions of X . The special subset $M_c \subseteq M_{fc}$ of fuzzy c partitions of X where in every u_{ik} is 0 or 1 is the discrete set of "hard," i.e., non-fuzzy c partitions of X . M_c is the solution space for conventional clustering algorithms. The fuzzy c -means algorithm uses iterative optimization to approximate minima of an objective function which is a member of a family of fuzzy c -means functional using a particular inner product norm metric as a similarity measure on $R^P \times R^P$. The distinction between family members is the result of the application of a weighting exponent m to the membership values used in the definition of the functional.

Definition: Let $U \in M_{fc}$ be a fuzzy c partition of X , and let v be the c tuple (v_1, v_2, \dots, v_c) , $v_i \in R^P$. The fuzzy c -means functional $J_m : M_{fc} \in R^P \rightarrow R^+$ is defined as:

$$J_m = \sum_{k=1}^n \sum_{i=1}^c (u_{ik})^m (d_{ik})^2 \quad (15)$$

Where, $U \in M_{fc}$ is a fuzzy c partition of X :

$$v = (v_1, v_2, \dots, v_c) \in R^{cp} \quad (16)$$

With $v_i \in R^P$ the cluster center or prototype of class i , $1 \leq i \leq c$, and

$$d_{ik}^2 = \|x_k - v_i\|^2 \quad (17)$$

$\| \cdot \|$ is any inner product norm metric which defines the Euclidian distance, and $m \in [1, \infty]$. The Euclidian distance [21] is used to calculate the distance between cluster centroid to each object. Let us use Euclidean distance, and then the distance matrix at iteration 0 is

$$D = \begin{bmatrix} A_1 & B_1 & C_1 & D_1 \\ A_2 & B_2 & C_2 & D_2 \end{bmatrix} \begin{bmatrix} x \\ y \end{bmatrix} \quad (18)$$

Each column in the distance matrix symbolizes the object. The first row of the distance matrix corresponds to the distance of each object to the first centroid and the second row is the distance of each object to the second centroid. For example, distance from medicine $C = (x, y)$ to the first centroid $c_1 = (A_1, A_2)$ is $(x - A_1)^2 + (y - A_2)^2$, and its distance to the second centroid $c_2 = (B_1, B_2)$ is $(x - B_1)^2 + (y - B_2)^2$, etc.

Note the several parameters in the definition of the fuzzy c-means functional. The squared distance is weighted by the m^{th} power of the membership of datum x in cluster i . Thus, J_m is a squared error criterion, and its minimization produces fuzzy clusters (matrix U) that are optimal in a generalized least squared errors sense.

The FCM algorithm, via iterative optimization of J_m , produces a fuzzy c partition of the data set $X = \{x_1, \dots, x_n\}$. The basic steps of the algorithm are given as follows ([18] for the derivation).

- 1) Fix the number of clusters c , $2 \leq c \leq n$ where $n = \text{number of data items}$. Fix, m where, $1 < m < \infty$. Choose any inner product induced norm metric $\| \cdot \|$ e.g., $A \in W_{pp}$ positive definite.
- 2) Initialize the fuzzy c partition $U^{(0)}$,
- 3) At step b , $b = 0, 1, 2, \dots$,
- 4) Calculate the c cluster centers $\{v_i^{(b)}\}$ with $U^{(b)}$ and the formula for the i^{th} cluster center:

$$v_{il} = \frac{\sum_{k=1}^n (u_{ik})^m x_{kl}}{\sum_{k=1}^n (u_{ik})^m}, \quad (l = 1, 2, \dots, p) \quad (19)$$

5) Update, $U^{(b)}$: calculate the memberships in $U^{(b+1)}$ as follows. For $k = 1$ to n ,

a) Calculate, I_k and \tilde{I}_k :

$$\begin{aligned} I_k &= \{i \mid 1 \leq i \leq c, d_{ik} = \|x_k - v_i\| = 0\}, \\ \tilde{I}_k &= \{1, 2, \dots, c\} - I_k, \end{aligned} \quad (20)$$

b) For data item k , compute new membership values:

i) if $I_k = 1$

$$u_{ik} = \left[\sum_{j=1}^c \left\{ \frac{d(x_k, v_j)}{d(x_k, v_i)} \right\}^{\frac{2}{m-1}} \right]^{-1} \quad (21)$$

ii) else, $u_{ik} = 0$ for all $i \in I_k$ and $\sum_{i \in \tilde{I}_k} u_{ik} = 1$; next k .

6) Compare $U^{(b)}$ and $U^{(b+1)}$ in a convenient matrix norm; if $\|U^{(b)} - U^{(b+1)}\| \leq \varepsilon$, where $\varepsilon = \{0 \text{ to } 1\}$, stop; otherwise, set $b = b + 1$, and go to step 4.

Use of the FCM algorithm requires determination of several parameters, i.e., c , ε , m , the inner product norm $\| \cdot \|$, and a matrix norm. In addition, the set $U^{(0)}$ of initial cluster centers must be defined. Although no theoretical basis for choosing a good value of m is available, $1 \leq m \leq 5$ is typically reported as the most useful range of values. Further details of computing protocols, empirical examples, and computational refinements are summarized elsewhere [20].

The point of attack below is to reduce the computational burden imposed by iterative looping between equation (15) and (16) when c , p , and n are large. It is this task to which the method now turns.

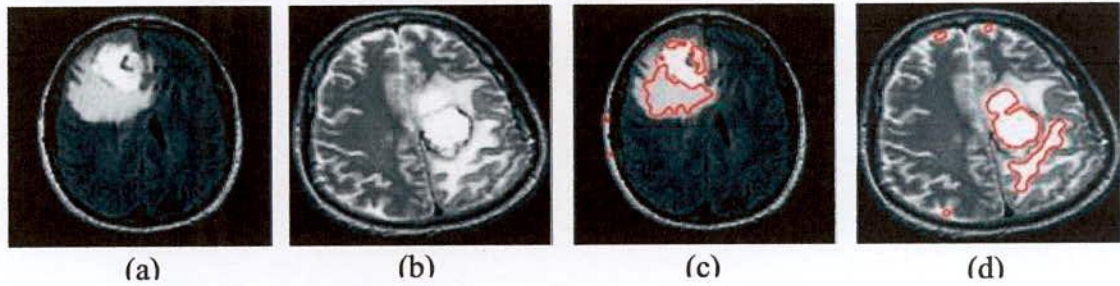


Figure 4.8: FCM based Brain MRI tumor detection (a, b) Original Brain MRI image and (c, d) FCM based segmented image.

In the following section the FCM based segmented image is shown in Figure. 4.8. In this (a) and (b) show the original MRI image of brain tumor where the tumor exist. Then 1st segmented image tumor is not detected correctly in (c) and in 2nd segmented image shown in (d), there is some blur with tumor.

In the FCM there are some limitations for the detection and proper segmentation which can be mentioned as below:

- ✓ FCM is noise sensitivity and imperfection to the abnormality of brain i.e. tumor, edema, and cyst.
- ✓ Blurred image is obtained if there is inhomogeneity of the brain image is found.

4.3 Summary

For accurate diagnosis of brain tumor patients, proper segmentation method is required to be used for MR images to carry out an improved diagnosis and treatment. Currently, information is provided by many images from various slices required for accurate diagnosis, planning and treatment purpose. The volume of the available information requires computation processing to inform the decision-making.

Now-a-days, speed of computation is no longer an issue for researchers. Therefore, the focus is directed toward improvement of information from images obtained through the slice orientation and perfecting the process of segmentation to get an accurate picture of the brain tumor.

In this chapter, some of the worthwhile recent research works done on brain tumor detection and segmentation are attempted to review. Through analysis of the literature, it is found that automation of brain tumor detection and segmentation from brain MR images is one of the most active research areas and enormous research has been done in this area for the last many years. However, currently there is no clinically accepted automated method.

CHAPTER 5

TKFCM Scheme for Tumor Detection

Chapter Outlines

- ❖ Introduction
- ❖ TKFCM Algorithm & Mathematical Model for Tumor Detection
- ❖ Results and Performance Analysis
- ❖ Summary

TKFCM Scheme for Tumor Detection

5.1 Introduction

The uprising world of medical science has brought new collection of inventions which make our domestic health life so fruitful. For designing a new method of tumor detection it is required to investigate the existing conventional process of tumor detection, while the limitations are to find out easily through previous chapter. Among them computational technique of detecting tumor in our brain is the most important part of new era of invention. As the brain contains most of the control of our body, so the detection of tumor which cause hilarious problem is needed to be good care [2]. For the MRI imaging technique, the gray image of brain tumor with little variation of gray level intensity is a cause of the misdetection of tumor for the expert. It can be easier either there be any computational technique of segmentation which makes the expert to detect the tumor in brain MRI image or there is a method through which the tumor is detected automatically. There are several techniques for the detection of tumor in brain MRI image discussed in [14]-[18]. Due to their limitation there is a scope of proposing an algorithm to eradicate their limitations.

In the following section the results of the proposed algorithm namely Template based K-means and modified Fuzzy C-means clustering (TKFCM) will be discussed in briefly, which can be used to mitigate the aforementioned requirement.

5.2 TKFCM Algorithm for Tumor Detection

Firstly, an MRI image is taken from the database which is made using MATLAB through the brain MRI images collected from [79]-[81]. This image is incorporated with tumor finding with MRI technique. The K-means algorithm is used to segment this MRI images on the basis of gray level. This gray level is selected depending on the temper of the image. Then the modified Fuzzy c-means algorithm which depends on the updated membership is applied to segment the template based K-means segmented image. The membership of modified Fuzzy c-means is updated with the cluster distances from centroid defining by the features of the tumor MRI image.

The proposed algorithm is integration of the K-means and Fuzzy c-means with some modification. The template is added along with the conventional K-means, which is identified by the temper or gray level intensity in the brain image. Besides, the Fuzzy c-means membership and Euclidian distance is modified by the image features.

Here, the coarse image $B(x_i, y_j)$ which is marked in describing desired template for the K-means could be found through convolution of temper based template and image shown in below equation (22):

$$B(x_i, y_j) = \sum_{i=n+1}^{M+n} \sum_{j=n+1}^{N+n} P(x_i, y_j) \oplus T_{MN(resize)} \quad (22)$$

Template based window is selected by T_{MN} which is given as:

$$T_{MN} = \sum_{i=n+1}^{M-n} \sum_{j=n+1}^{N-n} P(x_i, y_j) \quad (23)$$

In the equation (23), there is an temper based image matrix with number of gray level intensity, G and number of bins, S which is used to detect the temper of the image $P(x_i, y_j)$. Where the n is defined as $n = (winsize - 1) / 2$. With exact value of the temper, row and column, the desired temper is obtained.

In the Fuzzy C-means, $U_{ij}^{(m)}$ is the partition matrix with membership function whose value updated with Euclidian distance $d(x, v)$ which relies on the image features $F = \{F_1, F_2, \dots, F_C\}$, degree of fuzziness m , and feature center $V = \{v_1, v_2, \dots, v_i, \dots, v_C\}$ is expressed as:

$$U_{ij} = \left[\sum_{k=1}^C \left\{ \frac{d(x_j, v_i)}{d(x_j, v_k)} \right\}^{\frac{2}{m-1}} \right]^{-1} \quad (25)$$

In the previous research works, this Euclidian distance was used based on only one features for example similarity [18], but in our proposed method this relies on features like contrast, homogeneity, entropy etc.

Clusters center from where the clusters position and tumor are detected can be defined as:

$$V_i = \frac{\sum_{j=1}^N (U_{ij})^m \times j}{\sum_{j=1}^N (U_{ij})^m} \quad \text{where, } (i = 1, 2, \dots, C) \quad (26)$$

Separately Template based K-means and modified Fuzzy c-means clustering algorithm for segmentation can be written in equation as below:

$$J_k = \sum_{i=1}^C \sum_{j=1}^K P_{ij} \|x_i - c_j\|^2 \quad (27)$$

$$J_m = \sum_{j=1}^N \sum_{i=1}^K (U_{ij})^m (d_{ij})^2 \quad (28)$$

Then, from the equation (27) and (28) the contour through which the exact location of and tumor portion in any image can be find is

$$J_{km} = \oint_c (J_k, J_m) \quad (29)$$

Where, M and N are the row and column of P_{ij} a binary image matrix. The centroid of the cluster, number of data points in clusters and number of cluster is defined by N , C and K respectively. In the equation (29) which shows a contour integral of Template based K-means image and updated membership based FCM image, where c is the contour value. The last portion of equation (29) is defined as modified Fuzzy C-means whose Euclidian distance is depended on the image features and the first portion is used as the conventional K-means algorithm, which is defined by the distance from each point to cluster center.

The following five features are extracted for the classifier as:

- a. Energy, $F_1 = \sum_{i=1}^G \sum_{j=1}^G |P(x_i, y_j)|^2$ Here, G , is the gray level co-occurrence matrix.
- b. Contrast, $F_2 = \sum_{n=1}^G n^2 \sum_{i=1}^G \sum_{j=1}^G |P(x_i, y_j)|$ and $|i - j| = n$
- c. Homogeneity, $F_3 = \sum_{i=1}^G \sum_{j=1}^G \frac{P(x_i, y_j)}{1 + |i + j|}$
- d. Entropy, $F_4 = \sum_{i=1}^G \sum_{j=1}^G P(x_i, y_j) (-\ln(P(x_i, y_j)))$
- e. Correlation, $F_5 = \sum_{i=1}^G \sum_{j=1}^G \frac{(x_i, y_j) \times P(x_i, y_j) - (\mu_x \times \mu_y)}{(\sigma_x \times \sigma_y)}$

The TKFCM algorithm for tumor detection can be summarized as follow:

1. Define, $n = (\text{winsize} - 1) / 2$ and image matrix, $P = \sum_{i=1}^M \sum_{j=1}^N P(x_i, y_j)$
 2. Initialize template, $T_{MN} = \sum_{i=n+1}^{M-n} \sum_{j=n+1}^{N-n} P(x_i, y_j)$
 3. Determine coarse image, $B(x_i, y_j)$ from template, T_{MN}
 4. Reshape template based K-means segmented image

$$P_1 = \sum_{i=1}^C \sum_{j=1}^K P_{ij} \|x_i - c_j\|^2 \oplus \sum_{i=1}^M \sum_{j=1}^N B(x_i, y_j)$$
 5. Repeat step 2 to 4 until $T_{mn} \leq \sum_{k=1}^G \sum_{l=1}^S [T_{mn}(k) - T_{mn}(l)]$
 6. Post process the P_1
 7. Determine cluster centroid, C and degree of fuzziness, m .
 8. Initialize membership $U_{ij}^{(0)}$ of FCM
 9. Calculate cluster center, $v_i^{(l)} \Leftrightarrow U_{ij}^{(l)}, (i=1, 2, \dots, C)$ and $(l=0, 1, 2, \dots)$
 10. Determine image features, $F(x_j, v_i^{(l)}) \Leftrightarrow v_i^{(l)}$
 11. Update $U_{ij}^{(l)}$ with $d(x_j, v_i^{(l)})$ until $\|U_{ij}^{(l)} - U_{ij}^{(l+1)}\| \leq \epsilon, \epsilon = \{0 \text{ to } 1\}$
-

The whole method that has been proposed for the detection of tumor in brain MRI image using template based K-means and modified Fuzzy C-means is described by the following flow chart in Figure 5.1. In this flow chart firstly there is manipulated acquisition of brain MRI image, and then it is processed and given at the input of template based K-means segmentation method. Finally from the modified Fuzzy C-means with updated membership the detected tumor with red line marked is obtained. This is done through the clustered image which is automatically selected from the image features.

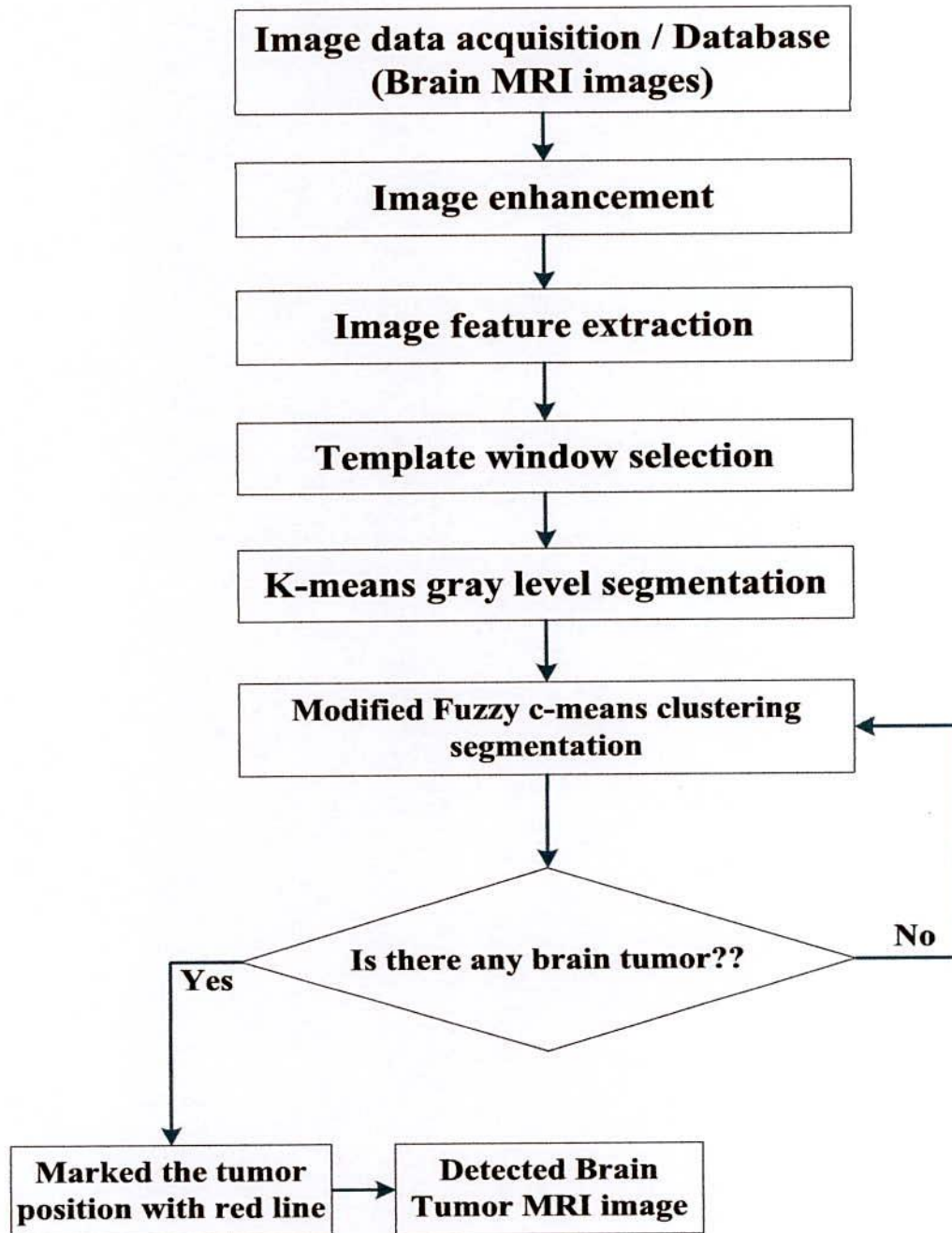


Figure 5.1: The flowchart of proposed TKFCM algorithm for tumor detection.

5.3 Results and Performance Analysis

There is a database of 40 brain tumor images shown in Figure 5.2. For the database some of the complex brain tumor images are obtained from the experimental images given by some renowned medical university and website in [79-81] for open use. These images are raw and blurred that is why it is needed to be processed and made usable for the detection. This is done through some algorithm of pre-processing under MATLAB software. As the images are very complicated to understand for the experts so there is a proposed computed diagnostic method for the detection discussed in section 5.2. In the following section the obtained results are shown and analyzed on their characteristics.

There is some steps which is used for the processing of the image as the input image was blurred. First the input image is adjusted and enhanced then, the image is threshold based linearization. This morphological operation is used for processing of the image. The comparison of enhanced and morphological image comprehends the feature of these images. These steps are shown in Figure 5.3.

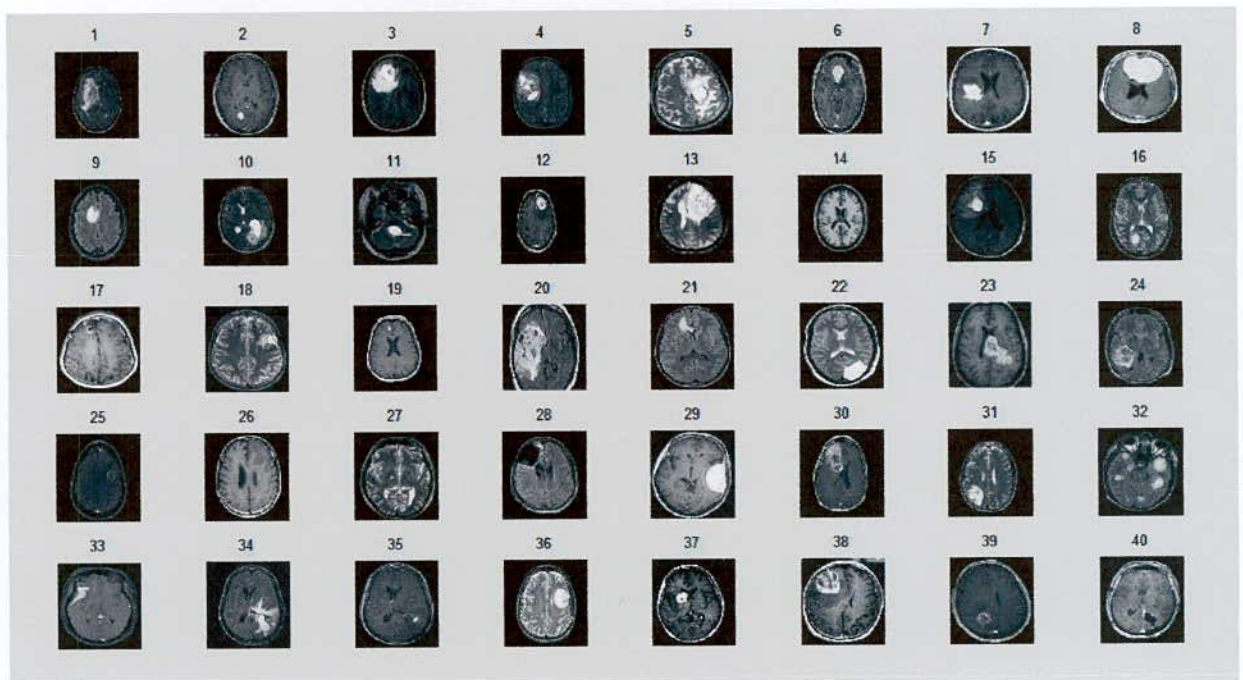


Figure 5.2: The database of 40 brain tumor MRI image

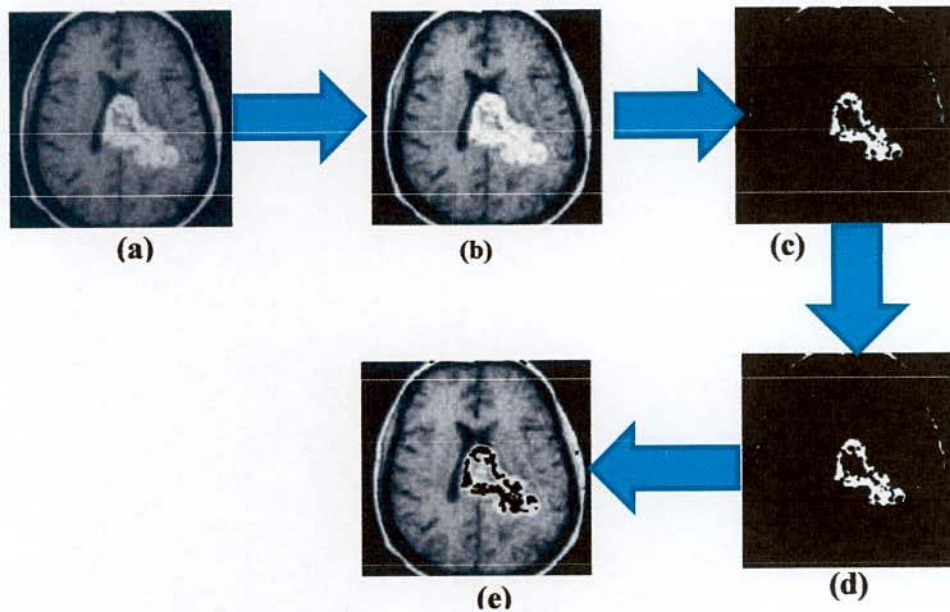


Figure 5.3: The pre-processing steps of the TKFCM, where (a) original brain mri image (b) enhanced brain mri image (c) thresh-holding image (d) morphological image (e) comparison of enhanced and morpholoical image

The tumor in these images is so critical that it is difficult for the common people to identify it so easily. In this TKFCM algorithm 3, 5, 9, 10, 15, 16, 18, 21, 27, 40 number images of database are used to detect the tumor position is shown in Figure 5.4 (a&d). A small portion of the brain tumor is not avoided. The input image is firstly processed through some filter. Then in Figure 5.4 (b&e), there is the first segmentation of the image using template K-means (TK). In which images are segmented based on their gray level intensity and temper of color of the original image. After that the tumor is detected and marked as red line in Figure 5.4 (c&f) using modified Fuzzy c-means (FCM) algorithm. In the FCM the membership function is updated on the basis of euclidian distance from cluster centre to each data point which mostly depends on the different features discussed in section 5.2. This could be significant to understand the importance of this proposed modified and incorporated method.

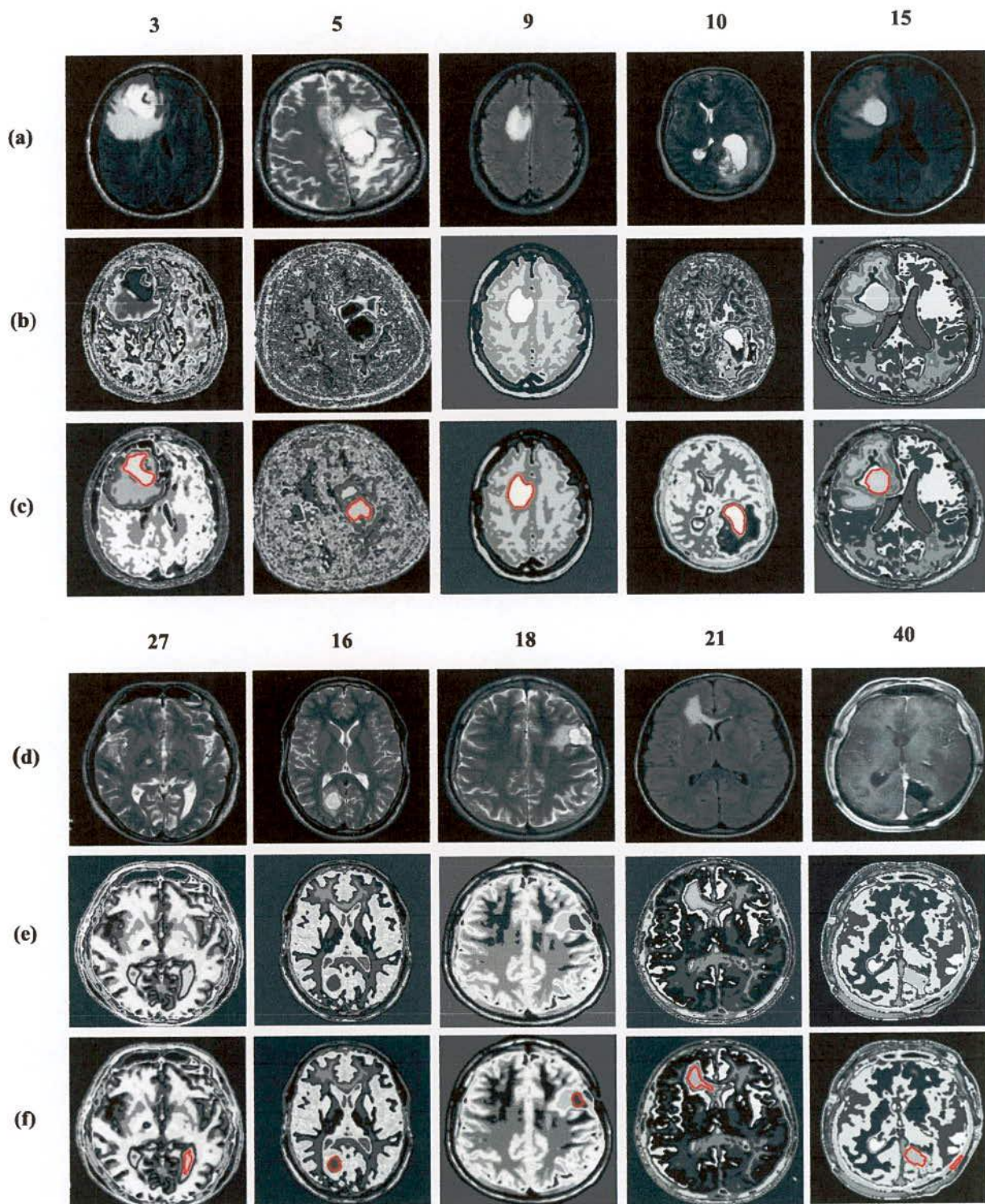


Figure 5.4: Enhanced Input images for TKFCM in (a & d), Segmented images from the 1st segmented algorithm (Template based K-means) in (b & e), Detected brain tumor images from the TKFCM in (c & f).

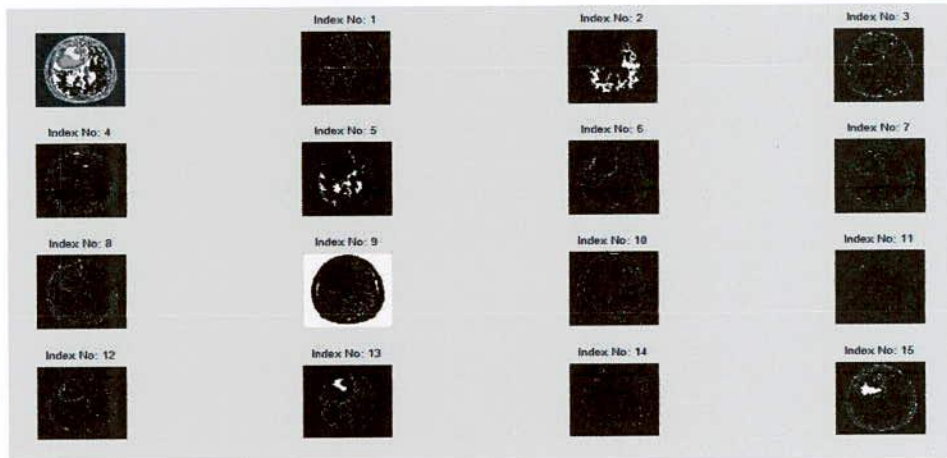


Figure 5.5: Several clustered images for input image no. 3.

On the basis of gray level intensity the modified FCM is performed for 15 clusters. Clustered image is referred as the image with its smallest gray level and separated from each other with their consecutive color intensity. For example, several clustered images for input image number 3 are shown in Figure 5.5. Here, the tumor portion with other portion of the image are shown in separate image, from this on the basis of the feature the tumor is selected. That is why, for image number 3 the index number 13 of Figure 5.3 is selected automatically and marked as red line for the tumor in Figure 5.4.

The network by which the performance of this technique is to measure through Neural Network is shown below Figure 5.6. The network consists of 40 input vector layers, one hidden layer with 17 neurons, and one output layer. Usually the network is consists of three layers like input layer, hidden layer, and output layer. The input and output layer is user defend nevertheless hidden layer is selected on the basis of performance. Hidden layer can be one or more for the analysis, however it is required that in hidden layer the number of layer should be least numbered.

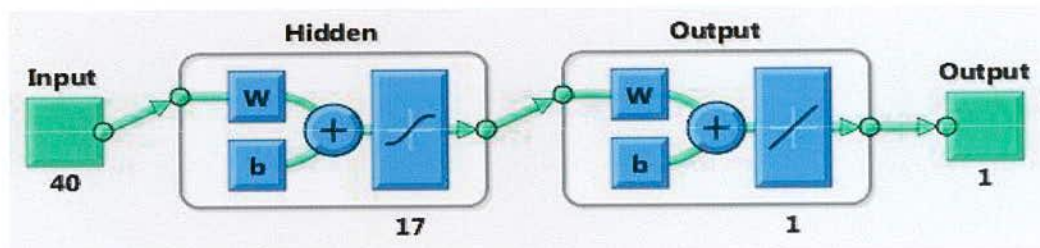


Figure 5.6: The Neural Network architecture.

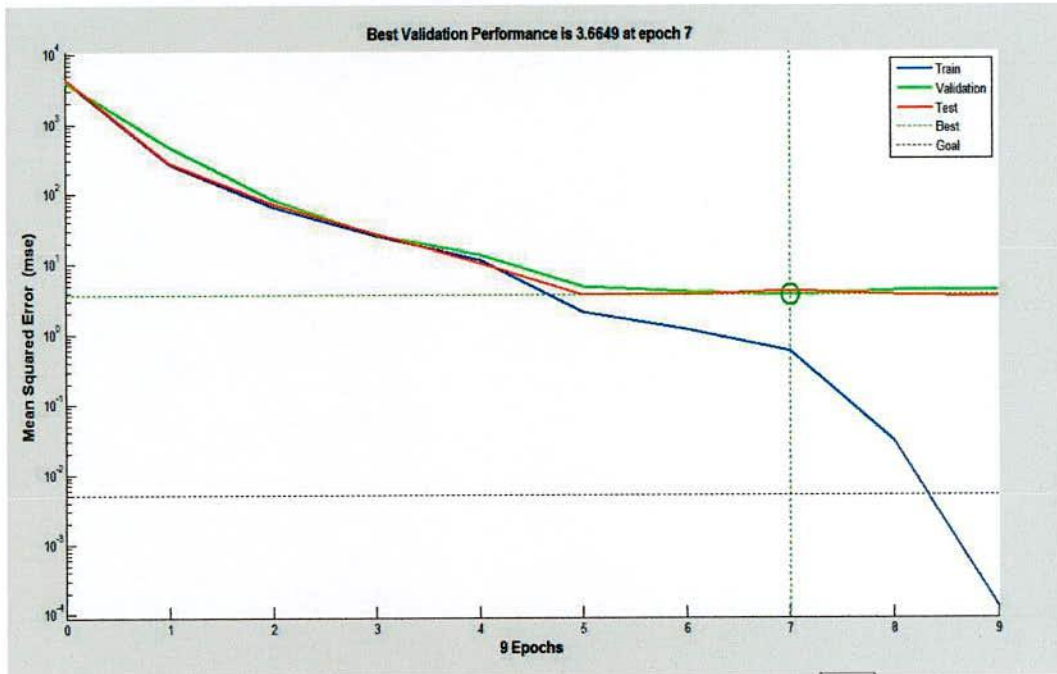


Figure 5.7: The performance curve for TKFCM method through neural network.

The performance curve shown in Figure 5.7 of the trained data, for number of iterations 60, increment number 0.05, performance goal or minimum error $0.5e-02$, minimum gradient $1e-10$, and maximum validation check failure 6. The performance goal is achieved between 8 and 9 iterations. Best validation performance is 3.6649 at iteration 7. The test data meets along with validation at its best values. The performance is depended on the value of least error, here in this analysis minimum error is used as 0.005 for the betterment of designed network. It is required that the number of iteration is least. The network has taken 9 iterations to meet the least error for the trained data of 40 images and mentioned criteria of the performance analysis.

Figure 5.8 shows curve of the parameters used for the analysis in graphically. In this, gradient is decreased and reached at descent value of 0.50474 at 9 iterations is described. Also, Levenberg-Marquardt optimization parameter (MU) decreases at its given values is mentioned. Besides, there is two best validation performances at 9 iteration. Again the MU value is increased and decreased then proceeds to the value of $1e-07$ at the 9 iterations. Finally there are 2 validation checks at the 9 epochs.

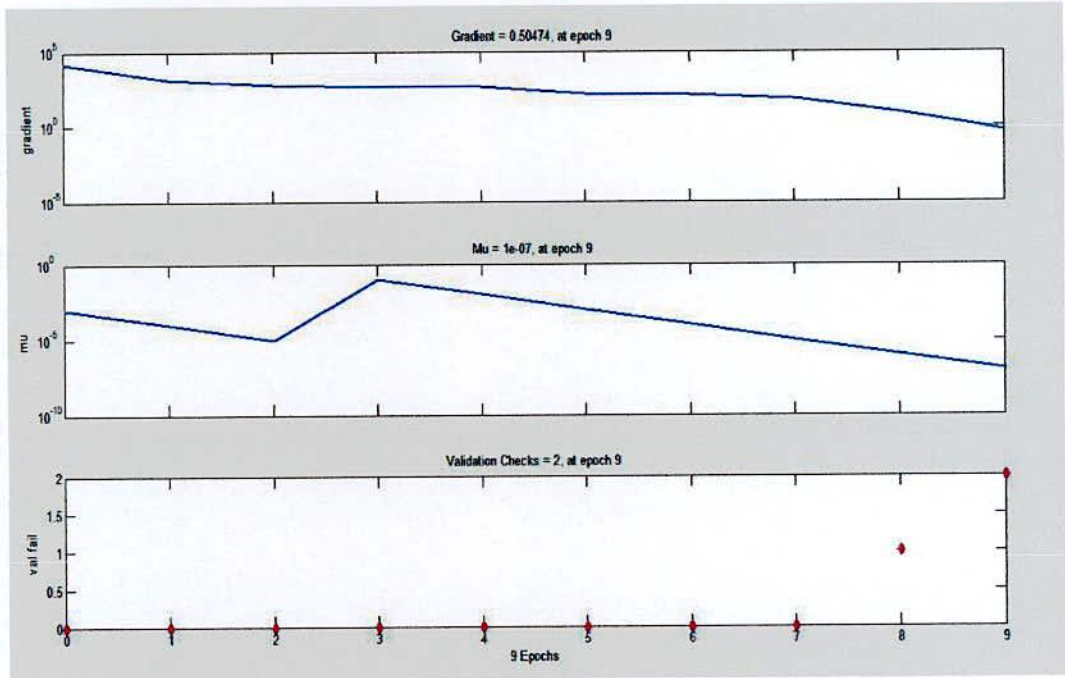


Figure 5.8: The Validation check, minimum gradient, and Mu curve for the network.

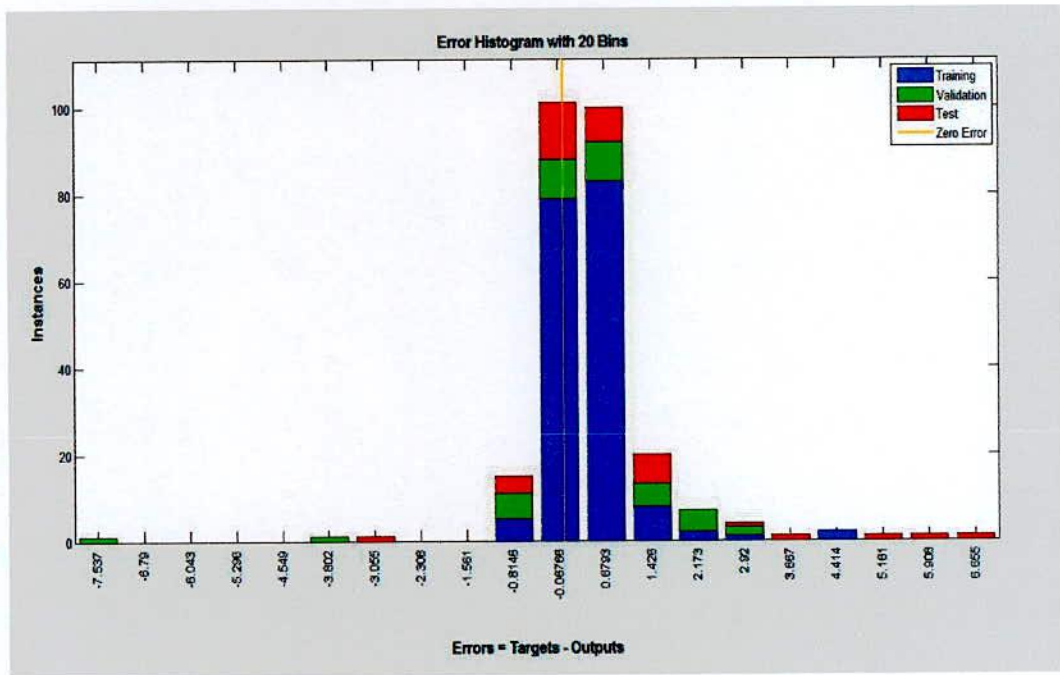


Figure 5.9: The Error histogram curve for the network.

The error histogram curve is described in Figure 5.9. The horizontal axis is belongs to the errors and vertical lines describes the number of instances for this errors. Where, the training, validation, test, and zero error are present. The zero error is shown by the yellow line because in that time the train, test and validation data are properly distinguished and the performance goal is achieved through the network. The train error is belonging from -0.8146 to 4.414 values. That means the train data between these values are appropriately trained with lest train errors. Same as zero error the green color is for validation errors and red color is defining the test errors.

The regression process of the training, validation, test and all data are preceded in the Figure 5.10. This shows that the regression to training is 0.99801, to validation is 0.9786, to test is 0.98108, and throughout all is 0.99307 which is so good. The curve describes how the data fit to the ideal regression line. The small circular values are the data. The dotted line is the ideal regression line. The full straight line with RGB color is regression curve of the designed network.

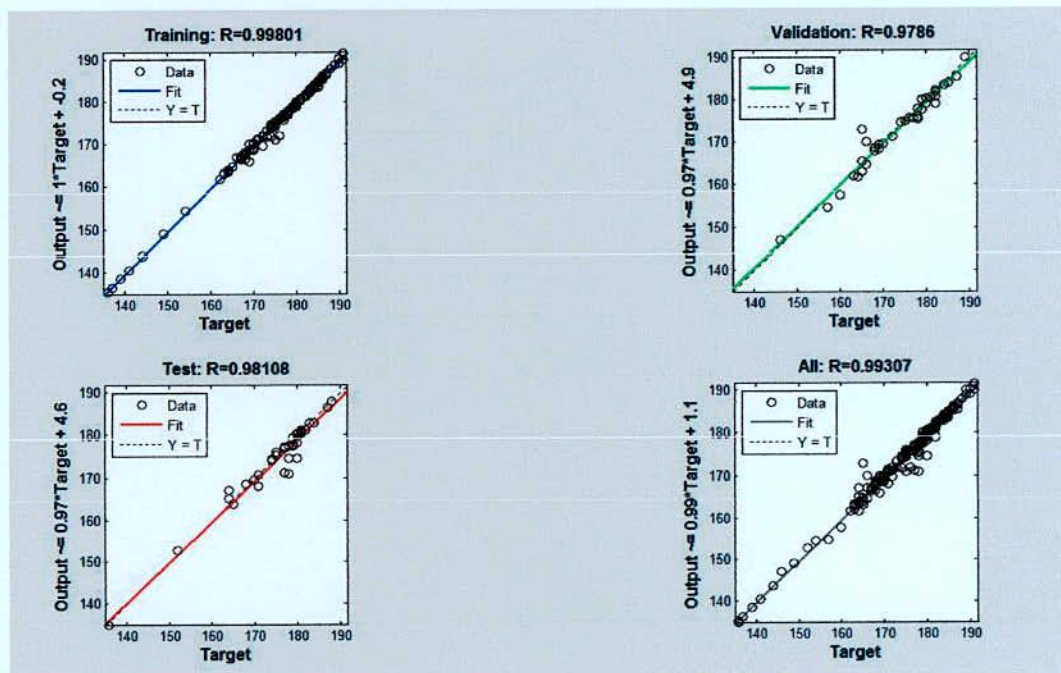


Figure 5.10: The regression curve for the network.

There is some error rate on the basis of identifying or not identifying any abnormal tissue in all brain tumor MRI image. This can be calculated depending on the value of true positive, false positive, true negative, and false negative [84]. The performance parameters can be calculated for the 40 brain tumor images through following

$$Sensitivity = \frac{TP}{(TP + FN)} \times 100 \quad (30)$$

$$Specificity = \frac{TN}{(TN + FP)} \times 100 \quad (31)$$

$$Accuracy = \frac{(TP + TN)}{(TP + TN + FN + FP)} \times 100 \quad (32)$$

Where, TP=True Positive, TN=True Negative, FP= False Positive, FN= False Negative

In Table 5.1 a comparison chart of parameter of performance analysis is elaborated among the conventional brain tumor detection processes with proposed TKFCM method. The performance analysis is comprehended through True Positive (TP), True Negative (TN), False Positive (FP), and False Negative (FN). On the basis of these values of performance measurement parameters the accuracy, sensitivity, and specificity are measure mathematically by using equation (30), (31), and (32). In the proposed TKFCM technique, there are 40 brain tumor images are taken as shown in Figure 5.2 and among them TP= 38, TN=1, FP=0, and FN=1.

Table 5.1: Parameters of performance analysis among conventional methods & TKFCM method [84]

Algorithms	TP	FP	TN	FN
Thresholding	20	5	9	6
Region Growing	26	2	10	2
Second order + ANN	21	2	16	1
Texture Combined +ANN	21	1	17	1
FCM	24	1	10	5
K-means	20	3	12	5
Proposed TKFCM	38	0	1	1

A comparison among the conventional brain tumor detection processes and proposed method is prepared which is observed in Table 5.2. It can be observed that TKFCM performs better than other methods. Apart from other, proposed TKFCM method sensibly pursues for the all parameters to a distinguished value, which is required for the betterment of the experts. The accuracy for the 40 brain MRI tumor image is 0.975 whereas the Texture combined +ANN is 0.95 so the difference is 0.025. From this analysis it can be said that for this database in Figure 5.2 the proposed method shows better performance in point of tumor detection in brain MRI image.

Table 5.2: Comparison among the conventional methods & TKFCM method

Algorithms	Sensitivity (%)	Specificity (%)	Accuracy (%)
Thresh-holding	76.9	64.25	72.5
Region Growing	92.8	83.3	90
Second order + ANN	95.5	88.8	92.5
Texture Combined +ANN	95.45	94.44	95
FCM	82.7	90.9	85
K-means	80	80	80
Proposed TKFCM	97.43	100	97.5

Again, the computational time require for detecting each tumor image is 140-150sec, by using the MATLAB2014a under operational environment of Core2duo processor, 2GB RAM, and windows 7 is better than other methods. A comparison of computational times among the Conventional Methods & TKFCM Method is shown in Table 5.3. In this conventional K-means, region growing, thresholding show more computational time. Again huge training data cause a greater computational time. Though conventional FCM shows less time, than proposed method but considering the performance this slight computational time is negotiable.

Table 5.3: Comparison of computational time among the conventional methods & TKFCM method

Algorithm	Computational time
Thresholding	~3 min
Region Growing	~10 min
ANN	~7-15 min
K-means	~4 min
FCM	~130-140 sec
Proposed TKFCM	~140-150 sec

5.4 Summary

The brain tumor detection is now a vital issued for the human being. This chapter has introduced a proposed method which will be beneficial to the experts. This chapter is included these following subjects:

- ✓ TKFCM algorithm for tumor detection is proposed. There was some limitation of the conventional methods which is mitigated through this proposed algorithm.
- ✓ A straightforward mathematical model is represented for the proposed TKFCM which is helpful to understand the algorithm.
- ✓ Step by step algorithm is specified as in the proceeding section after mathematical model.
- ✓ The proposed method and it evaluation is presented as a flow chart for the betterment of the readers.
- ✓ The important finding through TKFCM scheme is discussed and analyzed in the results and performance analysis section. The scheme is applied to 40 different brain tumor MRI image.
- ✓ The features are extracted and the values are used for the detection of tumor through proposed scheme.
- ✓ The performance of the proposed method is justified through the overall recognized neural network. There corresponding Figures 5.7, 5.8, 5.9, and 5.10 are shown which are cooperative in further research.
- ✓ Finally, the comparison of the proposed and conventional techniques is presented in Table 5.1, 5.2 and 5.3 where it describe that this scheme is better than other method in some aspects.

CHAPTER 6

TKFCM Scheme for Tumour Classification

Chapter Outlines

- ❖ 6.1 Introduction
- ❖ 6.2 TKFCM Algorithm & Mathematical Model
- ❖ 6.3 Results and performance analysis
- ❖ 6.4 Summary

TKFCM Scheme for Tumor Classification

6.1 Introduction

The brain comprehends complex structure which is so connected with the other parts of human body. The brain tumor that can paralyze human body either totally or partially is of different types. The brain tumor is not only a threat to human body but also to the other parts. Some of the tumors are just like normal tumors which are not harmful to the other parts but some are so harmful that causes death to the patients. So, perfect classification of the tumors can be efficient for the experts to be conscious about their effects. The previous chapter is used to describe the tumor detection process using TKFCM. This is helpful for the tumor classification.

Some works describes only for tumor classification in [20], [23]-[25]. Due to having several limitations, aforesaid individual method cannot be used properly to detect tumor as well as its stages. That is why a common technique is required for both detecting and classifying tumor and its stages simultaneously.

6.2 TKFCM Algorithm for Tumor Classification

The TKFCM algorithm and its mathematical model are elaborated at section 5.2 in chapter 5. The detected tumor is marked as red color in Figure 5.4. On the basis of their updated membership function in modified FCM the tumor is extracted by linearization algorithm on the basis of a gray level intensity based or temper based thresholding. The region properties algorithm is applied on morphological tumor image. The output of region properties algorithm is the combination of some characteristics parameters like Eccentricity, Perimeters, Bounding Box, Orientation, and Area. Among all these values of region properties only area is concerned and from this area values some conditional mode provides the tumor categories and its stages. The database is as same as in Figure 5.2, only difference is in the numbers. This database is consisted of 30 brain tumor MRI images.

The detected tumor is firstly thresholded and optimized on the basis of updated membership. Then the binary image is obtained through convolution of threshold and membership function is discussed in equation (21). The tumor area should have been taken as mean value neither it will show some error in determination of exact tumor area which proceed in misclassification.

From the convolution between level of thresholding, L_{th} and updated membership function $U_{ij}^{(l)}$ obtained from equation (25) in section 5.2, the binary black and white image (BW) is obtained,

$$BW = \sum_{i=1}^M \sum_{j=1}^N (U_{ij}^{(l)} \oplus L_{th}) \quad (33)$$

Where, i , and j are the pixel values of the binary image $p(x_i, y_j)$.

Then, applying region properties algorithm to BW , several characteristics parameters are obtained. These characteristics parameters are used to determine the area, eccentricity, orientation, bounding box, perimeters of the binary image of tumor. The standard area of normal and malignant tumor is obtained through [83]. The values are compared and decision of tumor categories is taken. The benign or normal tumor area range is different from malignant and stages of malignant tumor area are also varied from each other. The pixel values are converted to mm^2 by the equation of (35).

The TKFCM algorithm for tumor classification can be summarized as follow:

--

1. Define, $n = (\text{winsize} - 1) / 2$ and image matrix, $P = \sum_{i=1}^M \sum_{j=1}^N P(x_i, y_j)$
 2. Initialize template, $T_{MN} = \sum_{i=n+1}^{M-n} \sum_{j=n+1}^{N-n} P(x_i, y_j)$
 3. Determine coarse image, $B(x_i, y_j)$ from template, T_{MN}
 4. Reshape template based K-means segmented image

$$P_1 = \sum_{i=1}^C \sum_{j=1}^K P_{ij} \|x_i - c_j\|^2 \oplus \sum_{i=i+1}^M \sum_{j=j+1}^N B(x_i, y_j)$$
 5. Repeat step 2 to 4 until $T_{mn} \leq \sum_{k=1}^G \sum_{l=1}^S [T_{mn}(k) - T_{mn}(l)]$
 6. Post process the P_1
 7. Determine cluster centroid, C and degree of fuzziness, m .
 8. Initialize membership $U_{ij}^{(0)}$ of FCM
 9. Calculate cluster center, $v_i^{(l)} \Leftrightarrow U_{ij}^{(l)}, (i=1, 2, \dots, C)$ and $(l=0, 1, 2, \dots)$
 10. Determine image features, $F(x_j, v_i^{(l)}) \Leftrightarrow v_i^{(l)}$
 11. Update $U_{ij}^{(l)}$ with $d(x_j, v_i^{(l)})$ until $\|U_{ij}^{(l)} - U_{ij}^{(l+1)}\| \leq \epsilon, \epsilon = \{0 \text{ to } 1\}$
 12. Obtain the binary black and white image (BW) of updated $U_{ij}^{(l)}$
 13. From (BW) define area, eccentricity, perimeters and bounding box applying region properties algorithm.
-

--

As in chapter 5 the detection process is discussed in the section 5.2, so from that proposed process the tumor is detected. The detected tumor is marked as red color in Figure 5.4 in chapter 5. Then from this detected tumor the data is linearized and got the characteristics parameters using region properties algorithm. The characteristics parameter is used for the decision making for the tumor classification and stages identification. As here the normal tumor area belongs to (2-6) mm² and other standard values for different tumor are deliberated in Table 6.1 so, from there the tumor and its stages are verified and standardized for different brain tumor MRI images.

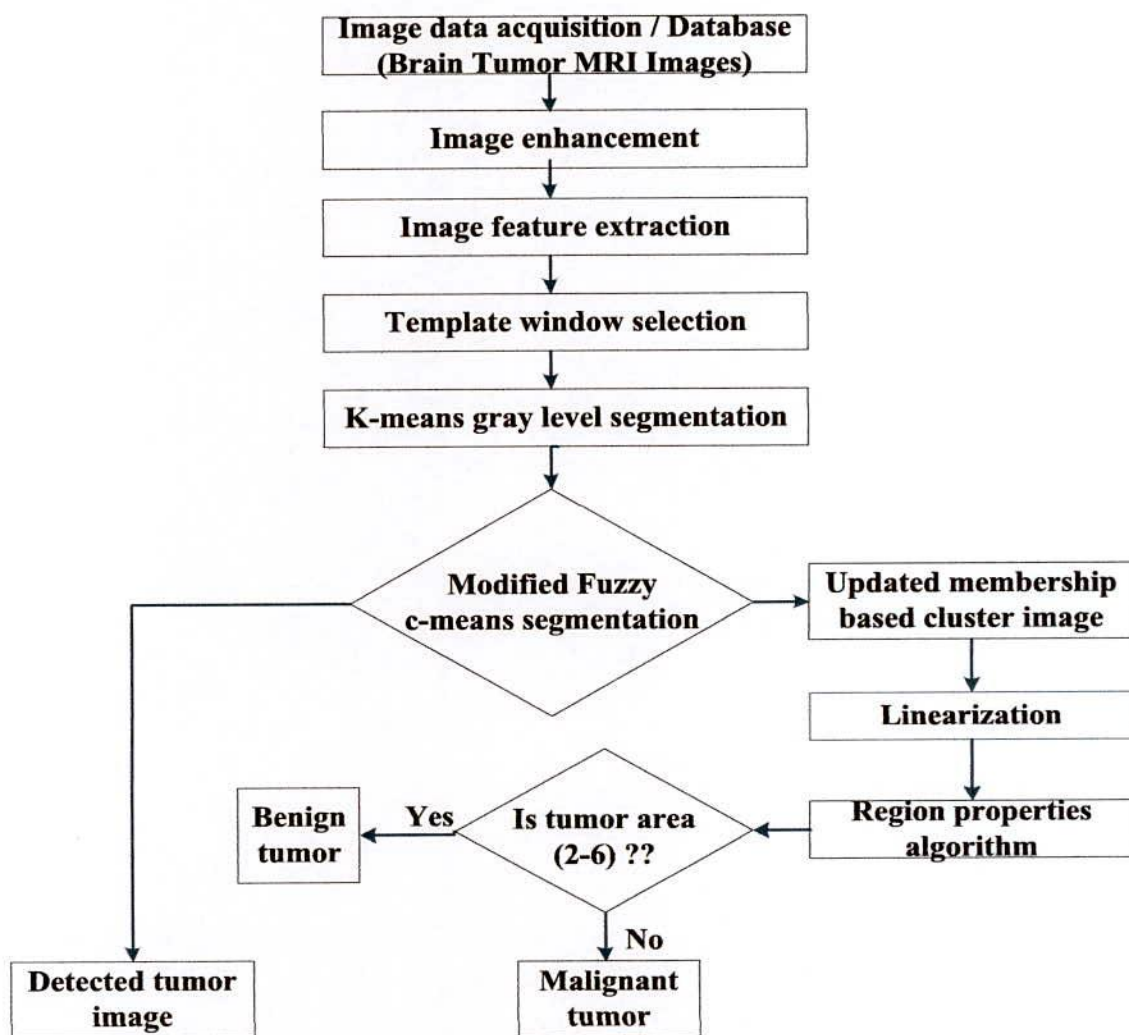


Figure 6.1: The flowchart of proposed TKFCM algorithm for brain tumor classification

6.3 Results and Performance Analysis

The database of 30 brain tumor images in Figure 6.2 is a collection of brain tumor images from [79-81]. The database is made usable through some preprocessing steps along with MATLAB, as the images of database provided by the renowned university website and oncology department webpage.

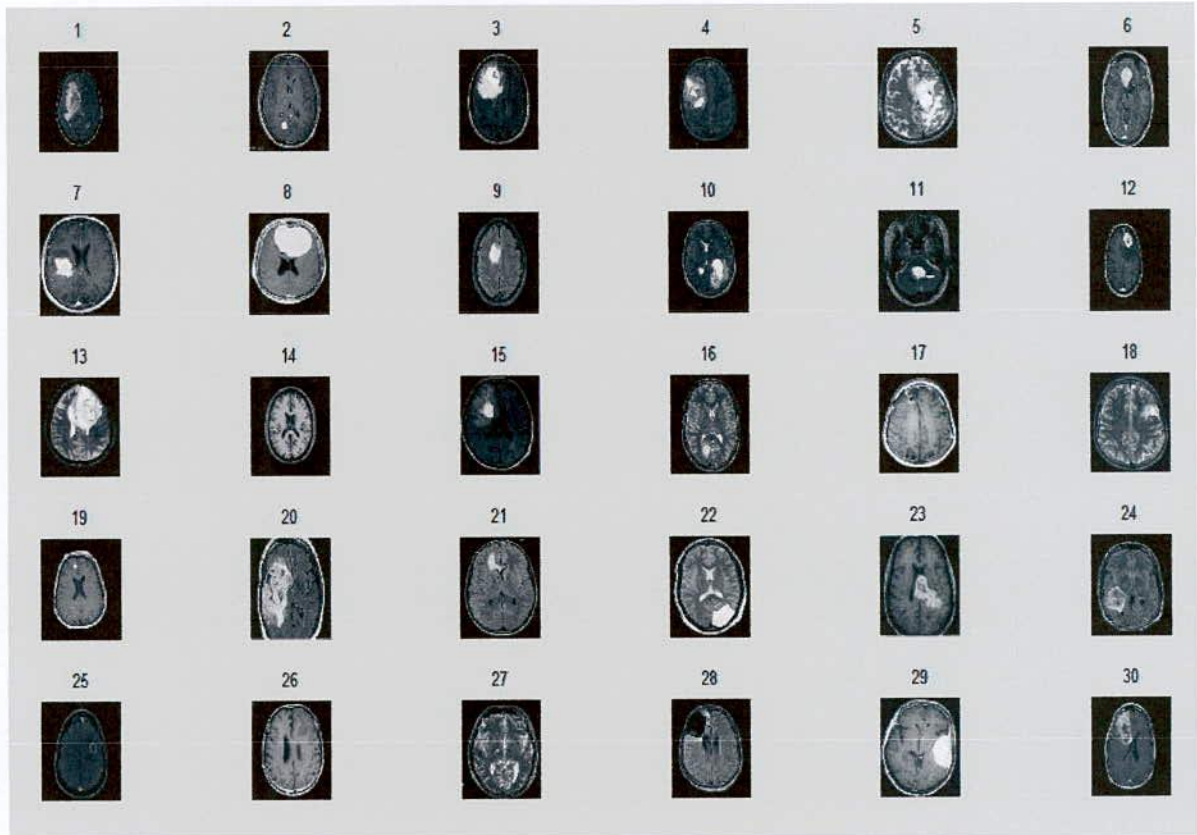


Figure 6.2 : The database of 30 brain tumor MRI image

On the basis of gray level intensity the modified FCM is performed for 8 clusters. The gray level image is segmented based on the temper or gray level intensity of the brain MRI images in Template based K-means algorithm discussed in section 5.2. The segmented image is separately divided and presented as each of the segmented portion as cluster. For example, several clustered images for input image number 3 are shown in Figure 6.3.

In this proposed TKFCM scheme these ten images numbered as 3, 5, 6, 8, 9, 13, 15, 18, 22, 29 respectively from database are used, for the classification of tumor and its area are shown in Figure 6.4. The Enhanced Input images for TKFCM are shown in Figure 6.4 (a & d), where the preprocessing steps of database images are done through Figure 5.3. In Figure 6.4 (b & e) the detected brain tumor images marked as the red color from the TKFCM are obtained. In this figure the tumor contour and clustered image is automatically selected and detected based on the feature values described in section 5.2. Classified brain tumor through linearization of TKFCM are presented in Figure 6.4 (c & f).. In which, the classification is provided by the application of level thresholding, updaed membership function, and region properties algorithm to the detected tumor.

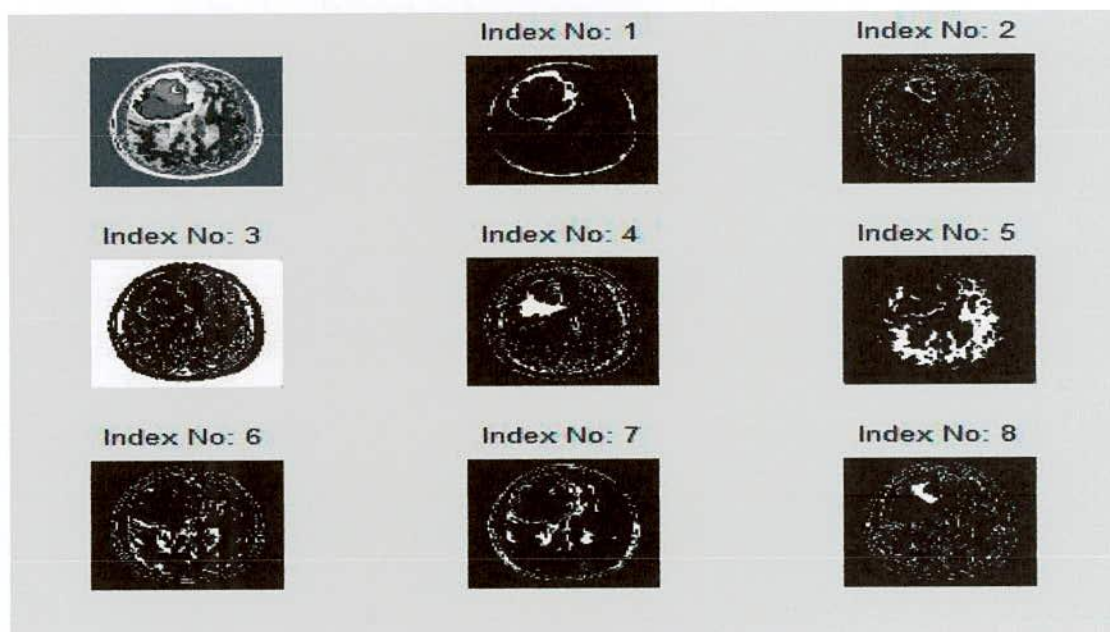


Figure 6.3: Several clustered images for input image number 3.

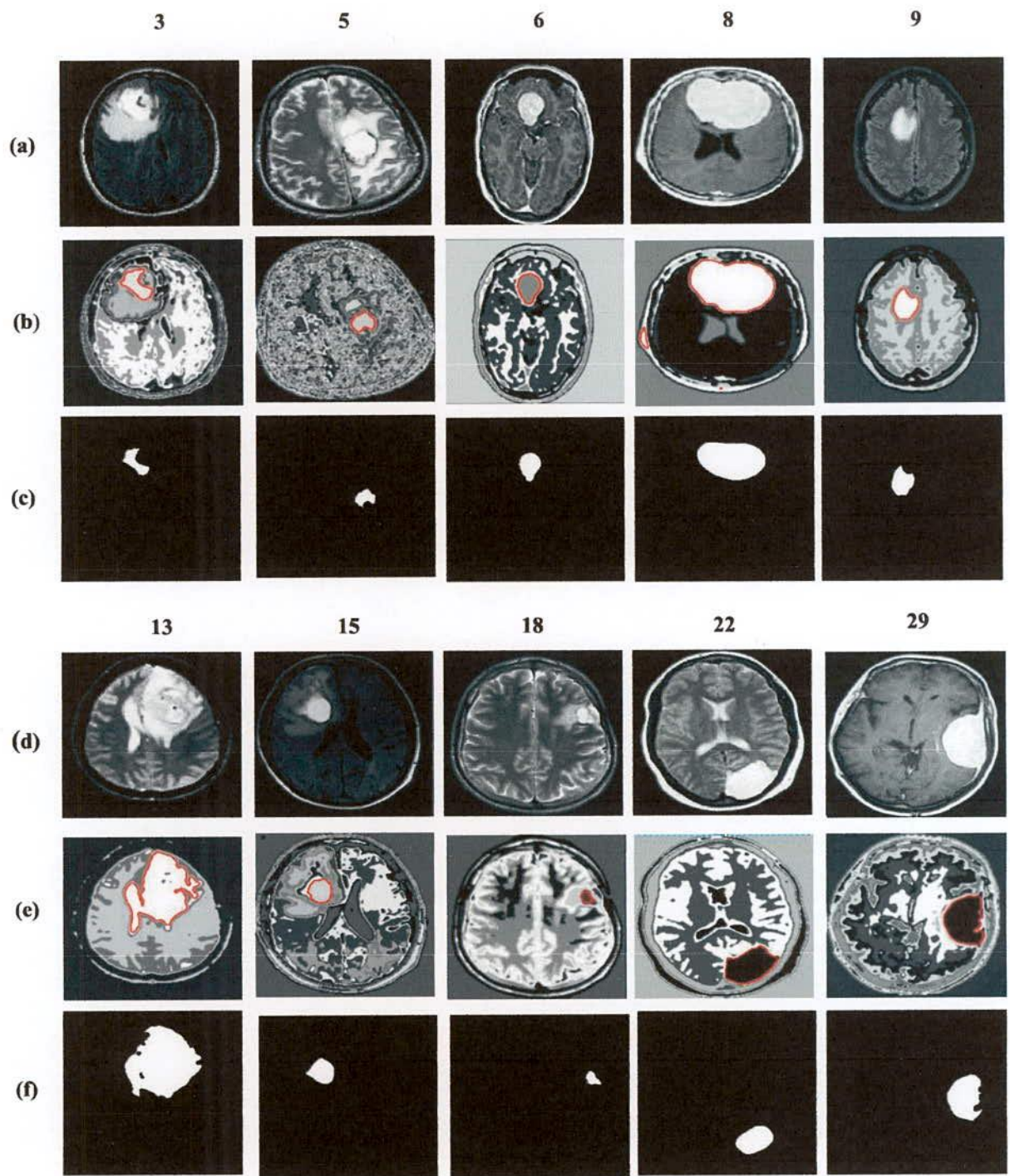


Figure 6.4: Enhanced Input images for TKFCM in (a & d), Detected brain tumor images from the TKFCM in (b & e), and Classified brain tumor through linearization of TKFCM in (c & f).

The tumor area is calculated using binary method. This implies that the image having only two values either 0 or 1 as black and white color respectively. The binary image can be calculated using equation (31) as a summation of total number of white and black pixels [21]:

$$I = \sum_{W=0}^M \sum_{H=0}^N [f(0) + f(1)] \quad (34)$$

Where black and white pixel are expressed as $f(0)$ and $f(1)$ respectively. The total pixel numbers of the image will be as follow:

$$Pixels = Width (W) \times Height (H) = 256 \times 256$$

The area is calculated through this formula:

$$Size\ of\ tumor, S = \left[(\sqrt{P}) \times 0.264 \right] mm^2 \quad (35)$$

where, Number of white pixel, $P = \sum_{W=0}^M [f(0)]$ and 1 Pixel = 0.264 mm .

Table 6.1: Standard area of the tumor classification

Types of Tumor	Standard area in mm ² [83]
Normal Tumor	(2-6)
Malignant stage I	(7-12)
Malignant stage II	(13-16)
Malignant stage III	(17-30)
Malignant stage IV	(>30)

Standard values of the different tumor classification are shown in Table 6.1. Here the tumor area varies from 2mm² to above 30 mm². The normal or benign tumor area belongs to (2-6) mm² collected from [83] for this database in Figure 6.2. The malignant tumor area is standardized in between 7 to above 30 mm². From this Table 6.1, the calculation of classified tumors is made easier to the common people.

The Table 6.2 show different characteristics parameters of brain tumor and classified tumor stages. The image number 5, 6, 9, 15, 18 illustrate the area are in between 2 to 6.1 mm², which is like the standard normal tumor area that is why, it belongs to benign tumor. On the other hand, other images like image numbered as 8, 13, 22, and 29 shows deliberately exaggerated area values more than normal tumor cause to detect malignant tumors with different stages. The area of the image number 22 belongs in between 7 to 12 mm² so this image is defined as *malignant stage I*. As like as number 8 the area of image number 29, 8, 13 are (13-16), (17-30), and (>30) mm² respectively. Then these images are defined as malignant stage II, II, and IV respectively.

Table 6.2: Calculation of Classified Tumors and of Its Stages

Image No.	Eccentricity	Perimeters	Bounding box	Orientation	Area in pixel	Area in mm ² (S)	Brain Tumor Stages
9	0.6511	122.730	[98.5 80.5 32 46]	87.9041	993	3.76	Benign: <i>Just like normal tumor</i>
6	0.7281	118.661	[104.5 55.5 32 46]	85.5539	1011	3.83	Benign: <i>Just like normal tumor</i>
15	0.3610	121.143	[66.5 67.5 41 41]	-50.3383	1098	4.16	Benign: <i>Just like normal tumor</i>
18	0.9565	12.463	[25.5 73.5 4 6]	65.7690	11	0.04	Benign: <i>Just like normal tumor</i>
5.	0.4924	78.1780	[141.5 117.5 23 27]	49.7918	534	6.1	Benign: <i>Just like normal tumor</i>
22	0.7598	158.806	[137.5 178.5 59 48]	27.8226	1882	7.13	Malignant: <i>Stage I spreading slowly</i>
29.	0.7489	219.517	[170.5 102.5 51 72]	84.7361	2592	13.44	Malignant: <i>Stage II (no lymph) spread wide</i>
8.	0.8113	249.884	[89.5 41.5 97 59]	8.6715	4522	17.75	Malignant: <i>Stage III spreading very fast</i>
13	0.4646	396.583	[87.5 23.5 110 114]	58.0054	8003	30.3	Malignant: <i>Stage IV spreading to other parts of body</i>

In Table 6.3, a comparison chart is prepared among the conventional brain tumor detection processes and proposed TKFCM method. The performance analysis is comprehended through True Positive (TP), True Negative (TN), False Positive (FP), and False Negative (FN). In proposed TKFCM technique there are 30 brain tumor images are taken and among them TP= 27, TN=1, FP=0, and FN=2. From the equation (30), (31), and (32) the sensitivity of 93.1%, 100% specificity and accuracy of 93.3% are obtained which is better than the conventional methods like thresholding, region growing, ANN, FCM, and K-means. As the ANN+ second order comprehends the value of accuracy of 92.2% but the specificity and sensitivity are not so good. But, proposed TKFCM method sensibly pursues for all parameters to a value, which is required for the betterment of the experts.

Table 6.3: Comparison among the conventional methods & TKFCM method

Algorithms	Sensitivity (%)	Specificity (%)	Accuracy (%)
Thresholding	84	80	83.3
Region Growing	88.46	75	86.7
Second order + ANN	91.42	90.1	92.22
FCM	87.5	85.7	87
K-means	82.3	92.85	83.3
Proposed TKFCM	93.1	100	93.3

Again, the computational time require for detecting each tumor image is ~200sec, by using the MATLAB2014a under operational environment of Core2duo processor, 2GB RAM, and windows 7 is better than other methods. A comparison of computational times among the Conventional Methods & TKFCM Method is shown in Table 6.4. In this conventional K-means, region growing, thresholding show more computational time. Again huge training data cause a greater computational time. Though conventional FCM shows less time, than proposed method but considering the performance of proposed method this slight computational time is negotiable.

Table 6.4: Comparison of computational time the conventional methods & TKFCM method

Algorithm	Computational time
Thresholding	~5-7 min
Region Growing	~10 min
ANN	~15 min
K-means	~5 min
FCM	~160-170 sec
Proposed TKFCM	~200 sec

6.4 Summary

If the chapter is summarized then there is some point which come forward which is briefly discussed in bellow section:

- ✓ In this chapter the linearized TKFCM algorithm for tumor and its stages classification is proposed. There was some limitation of the conventional methods which is mitigated through this proposed algorithm.
- ✓ A straightforward mathematical model is represented in section 5.2 which is preceded in section 6.2 for the proposed linearized TKFCM which is helpful to understand the algorithm.
- ✓ The algorithm is given as step by step in the preceding section 6.2 after mathematical model briefly described in section 5.2.
- ✓ A flow chart is used to describe the proposed method and it evaluation Figure 6.1.
- ✓ The results and performance analysis section is briefly discussed in section 6.3 about the important finding through TKFCM scheme. The scheme is applied to 30 different brain tumor MRI images.
- ✓ The classified tumor are presented in Figure 6.4.
- ✓ Characteristics parameters are obtained from the TKFCM scheme where, 10 brains MRI information is acquired and shown the Table 6.1 and 6.2 then, calculated the area of the tumor.
- ✓ Then decision of classifying the tumor and different stages are shown in the Table 6.2.
- ✓ Finally, the computational time and comparison of the proposed and conventional techniques is presented as Table 6.3 and 6.4 where it describes that this scheme is better than other in some aspects.

CHAPTER 7

Conclusions

Chapter Outlines

- ❖ Outcomes
- ❖ Limitations
- ❖ Application and Future work

Conclusions

7.1 Outcomes

In this thesis paper, two types of schemes for tumour detection and classification are proposed and their performances are analysed considering different categories of parameter in the previous chapters. There are some unique outcomes of these schemes through this thesis. In this section, these aftermaths are mentioned gradually which will show the total thesis work at a glance. The outcomes are following below.

- A new tumour detection scheme named by TKFCM scheme is proposed and its mathematical expression is explained.
- The process to reach the optimum segmentation by using the TKFCM is elucidated on the variation of features value of the brain MRI images.
- The concept of detecting the tumour with TKFCM algorithm is clarified through different universal and some new equations.
- A new style of Linearized TKFCM scheme is proposed with neat mathematical expression for tumour and its stages classification.
- The mathematical expression is presented as general form to reproduce it for feature values.
- Optimization technique of tumour detection and classification scheme is described on the basis of choosing the best set of characteristics parameter such as area, perimeter, eccentricity, bounding box, and orientation.
- The performance of this TKFCM scheme is analysed with neural network and compared with the conventional methods, and it is shown that the proposed scheme is optimum than that.
- These two proposed scheme is designed for not only the optimum segmentation of brain MRI but also the optimum utilization of tumour classification in further imaging techniques.

7.2 Limitations

In a computerized system different parameter need to be considered for the better performance. If it is a matter of human brain that is the main part of body then the perfect detection of existing brain tumour is necessary. The TKFCM scheme is proposed on the consideration of those all parameter for the segmentation. It is highly profound to the user if they are going to calculate the feature values of the tumour images. Sometimes there is some image which does not have efficient information for their image quality then it misleads the results of TKFCM.

Again, the linearized TKFCM scheme for tumour and its stages classification is one of the schemes which have mitigate some of the problem of thresh-holding, FCM, classifier and k-means algorithm in classification perception. This is to keep in mind that proper classification is obtained if and only if the characteristics parameters are acquired correctly. In linearized TKFCM this has clarified as there is a criterion of taking the mean value of the all characteristics parameters. There is a database of only 30 or 40 brain MRI images of similar kinds of tumor, but in practical the brain structure is complicated and it provides the ubiquitous tumor images. These types of tumor and a database of numerous images of complicated tumor can be difficult to detect using proposed TKFCM method

This TKFCM algorithm for detection and classification of tumour is used for the brain MRI image. In these kinds of images initially there is some problem to determining the standard value of the features and characteristics parameter provided by the certified institute. As the feature values for detecting tumor varies frequently for the complicated structure then it is required for the suggestion of experts.

7.3 Applications and Future work

These two TKFCM and linearized TKFCM schemes are able to cope itself for special purpose like tumor detection, drug designing, precautionary of tumor, tumor classification and automatic image processing etc. This factor can be varied according to the mathematical model of the proposed method to get the desired performances.

This TKFCM algorithm for detection and classification of tumor is used for the brain MRI image. In these kinds of images initially there is some problem to determining the standard value of the features and characteristics parameter along with thresh-holding as there is some blurred noise in actual image. This problem is eradicated with proper processing and filtering. So if the image quality is high then this technique can be made as universal for the computation based diagnostics. In the linearized TKFCM method only area values are used for tumor and its stages classification that is why it is limited to this database. In future, all the characteristics parameters should be considered for eradicating this problem. Then, this proposed method can be used for SPECT, PET, and CT along with neuro image segmentation and classification in further research.

References

- [1] J. Mendez, P. G. Tahoces, M. J. Lado, M. Souto, and J. J. Vidal, "Computer-aided diagnosis: Automatic detection of malignant masses in digitized mammograms," *Medical Physics*, vol. 25, pp. 957–64, June. 1998.
- [2] M. N. Ahmed, S. M. Yamany, N. Mohamed, and T. Moriarty, "A modified Fuzzy c-means algorithm for bias field estimation and segmentation of MRI data", *IEEE Transaction on Medical Imaging*, vol. 21, no. 3, pp. 193-199, March, 2002.
- [3] S. A. Narod, "Tumor size predicts long-term survival among women with lymph node-positive breast cancer," *Current Oncology*, vol. 19, no.5, pp. 249-253, October, 2012.
- [4] D. J. Hemanth, C. K. S. Vijila, and J. Anitha, "Application of neuro-Fuzzy model for MR brain tumor image classification," *Biomedical Soft Computing and Human Sciences*, vol. 16, no. 1, pp. 95-102, July, 2007.
- [5] H. Zhu, *Medical Image Processing Overview*, University of Calgary.
- [6] K. V. Leemput, F. Maes, D. Vandermeulen, and P. Suetens, "Automated model-based tissue classification of MR images of the brain," *IEEE Transaction on Medical Imaging*, vol. 18, no. 10, pp. 897–908, October, 1999.
- [7] R. Rana, H.S. Bhadauria, and A. Singh, "Study of various methods for brain tumor segmentation from MRI images," *International Journal of Emerging Technology and Advanced Engineering*, vol. 3, no. 2, pp. 338-342, June, 2013.
- [8] S. Shen, W. Sandham, M. Granat, and A. Sterr, "MRI Fuzzy segmentation of brain tissue using neighborhood attraction with neural-network optimization," *IEEE Transactions on Information Technology in Biomedicine*, vol. 9, no. 3, pp. 459 – 467, September, 2005.
- [9] N. Noreen, K. Hayat, and S. A. Madani, "MRI Segmentation through wavelets and Fuzzy C-Means," *World Applied Sciences Journal (Special Issue of Applied Math)*, vol. 13, pp.34-39, 2011.
- [10] D. L. Pham, C. Xu, and J. L. Prince, "Current Methods in Medical Image Segmentation," *Annual review on Biomedical Engineering*, vol.2, pp.315-337, 2000.

- [11] L. Lemieux, G. Hagemann, K. Krakow, and F. G. Woermann, "Fast, accurate, and reproducible automatic segmentation of the brain in T1-weighted volume MRI data," *Magnetic Resonance Medical Imaging*, vol. 42, pp. 127–135, 1999.
- [12] H. Suzuki and J. Toriwaki, "Automatic segmentation of head MRI images by knowledge guided thresholding," *Computed Medical Image Graphics*, vol. 15, no. 4, pp. 233–240, 1991.
- [13] R. M. Haralick and L. G. Shapiro, "Image segmentation techniques" *Computer Vision & Graphics Image Processing*, vol.29, pp.100–132, 1985.
- [14] A. R. Robb, *Biomedical Imaging, Visualization, and Analysis*. New York: Wiley, 2000.
- [15] R. Pohle and K. D. Toennies, "Segmentation of medical images using adaptive region growing," *Proceeding of SPIE—Medical Imaging*, vol. 4322, pp. 1337–1346, 2001.
- [16] T. Y. Law and P. A. Heng, "Automated extraction of bronchus from 3D CT images of lung based on genetic algorithm and 3D region growing," *Proceeding of SPIE — Medical Imaging*, vol. 3979, pp. 906–916, 2000.
- [17] W. M. Wells III, W. E. L. Grimson, R. Kikinis, and F. A. Jolesz, "Adaptive segmentation of MRI data," *IEEE Transaction on Medical Imaging*, vol. 15, no. 4, pp. 429–442, August, 1996.
- [18] L. O. Hall, A. M. Bensaid, L. P. Clarke, R. P. Velthuizen, M. S. Silbiger, and J. C. Bezdek, "A comparison of neural network and Fuzzy clustering techniques in segmenting magnetic resonance images of the brain," *IEEE Transaction Neural Network*, vol. 3, no. 5, pp. 672–682, September, 1992.
- [19] C. L. Li, D. B. Goldgof, and L. O. Hall, "Knowledge-based classification and tissue labeling of MR images of human brain," *IEEE Transaction Medical Imaging*, vol. 12, no. 4, pp. 740–750, April, 1993..
- [20] D. L. Pham and J. L. Prince, "Adaptive Fuzzy segmentation of magnetic resonance images," *IEEE Transaction on Medical Imaging*, vol. 18, no. 9, pp. 737–752, September, 1999.
- [21] W. Narkbuakaew, H. Nagahashi, K. Aoki, and Y. Kubota, "Integration of Modified K-means Clustering and Morphological Operations for Multi-Organ Segmentation in CT

- Liver-Images,” *Recent Advances in Biomedical & Chemical Engineering and Materials Science*, pp.34-39, March, 2014.
- [22] K. V. Leemput, F. Maes, D. Vandermeulen, and P. Suetens, “Automated model-based tissue classification of MR images of the brain”, *IEEE Transaction on Medical Imaging*, vol. 18, no. 10, pp. 897–908, October, 1999.
- [23] R. Oweis, and M. Sunna, “A combined neuro–Fuzzy approach for classifying image pixels in medical applications”, *Journal of Electrical Engineering*, vol. 56, no. 5-6, pp. 146–150, 2005.
- [24] H. R. Shally, and K. Chitharanjan, “Tumor volume calculation of brain from MRI slices”, *International Journal of Computer Science & Engineering Technology (IJCSET)*, vol. 4, no. 08, pp. 1126-1132, August, 2013.
- [25] R. N. Charles, L. Norman, R. Strominger, J. Demarest and D. A. Ruggiero, *The Human Nervous System: Structure and Function*, 6th edition, Humana Press, 2005.
- [26] www.teamrads.com/Cases/Neuroanatomy/MRI, Accessed on: January, 12, 2012
- [27] About brain tumors-a primer for patients and caregivers, American Brain Tumor Association, IL 60631, Chicago.
- [28] S. G. Narkhede, et al., *Int. Journal of Engineering Research and Application*, www.ijera.com, ISSN: 2248-9622, Vol. 3, Issue 6, pp.430-432, November-December, 2013.
- [29] J. C. Buckner, et al., “Central Nervous System Tumors”, *Mayo Clinic Proceedings*, Vol. 82, No. 10, pp. 1271-1286, 2007.
- [30] D. N. Louis, H. Ohgaki, O. D. Wiestler, and W. K. (Eds.) Cavenee, “WHO Classification of Tumors of the Central Nervous System”, *International Agency for Research on Cancer (IARC)*, Lyon, France, 2007.
- [31] *Brain Tumor Primer- A Comprehensive Introduction to Brain Tumors*, 9th Edition, American Brain Tumor Association
- [32] J. C. Bezdek, *Pattern Recognition with Fuzzy Objective Function Algorithms*, Kluwer Academic Publishers, USA, 1981.

- [33] R. Damadian, M. Goldsmith, and L. Minkoff, "NMR in Cancer: XVI. FONAR Image of the Live Human Body", *Physiological Chemistry and Physics*, vol. 9, no. 1, pp. 97- 100, 1977.
- [34] R. A. Novelline, and L. F. Squire, *Squire's Fundamentals of Radiology*, Harvard University Press, ISBN: 0674012798, 2004.
- [35] C. Westbrook, *MRI at Glance*, Blackwell Science Publishing, 2002
- [36] <http://www.radiologyassistant.nl/>, Accessed on: January, 12, 2012
- [37] *Medical Imaging in Cancer Care: Charting the Progress*, US Oncology and National Electrical Manufacturers Association (NEMA), Accessed on January 20, 2012 at http://www.healthcare.philips.com/pwc_hc/us_en/about/Reimbursement/assets/docs/cancer_white_paper.pdf
- [38] A. O. Rodriguez, "Principles of Magnetic Resonance Imaging", *Revista Mexicana de Fisica*, vol. 50, no. 3, pp. 272-286, 2004.
- [39] S. Prima, N. Ayache, T. Barrick, and N. Roberts, "Maximum Likelihood Estimation of the Bias Field in MR Brain Images: Investigating Different Modeling of the Imaging Process", *Processing of Medical Image Computing and Computer-Assisted Intervention (MICCAI' 2001)*, vol. 2208, pp. 811-819, 2001.
- [40] X. Li, L. Li, H. Lu, D. Chen, and Z. Liang, "Inhomogeneity Correction for Magnetic Resonance Images with Fuzzy C-Mean Algorithm", *Proceeding of SPIE*, vol. 5032, 2003.
- [41] S. Ruan, C. Jaggi, J. Xue, J. Fadili, and D. Bloyet, "Brain Tissue Classification of Magnetic Resonance Images Using Partial Volume Modeling", *IEEE Transactions on Medical Imaging*, vol. 19, no. 12, pp. 1179- 1187, 2000.
- [42] S. M. Larie and S. S. Abukmeil, "Brain abnormality in schizophrenia: a systematic and quantitative review of volumetric magnetic resonance imaging studies", *Journal of Psychology*, vol. 172, pp. 110–120, 1998.
- [43] P. Taylor, "Invited review: computer aids for decision-making in diagnostic radiology—a literature review", *British Journal for Radiology*, vol. 68, pp. 945–957, 1995.

- [44] A. J. Worth, N. Makris, V. S. Caviness, and D. N. Kennedy, "Neuroanatomical segmentation in MRI: technological objectives", *International Journal on Pattern Recognition and Artificial Intelligence*, vol. 11, pp. 1161–1187, 1997.
- [45] V. S. Khoo, D. P. Dearnaley, D. J. Finnigan, A. Padhani, S. F. Tanner, and M. O. Leach, "Magnetic resonance imaging (MRI): considerations and applications in radiotherapy treatment planning", *Radiotherapy Oncology*, vol. 42, pp. 1–15, 1997.
- [46] H. W. Muller-Gartner, J. M. Links, et al., "Measurement of radiotracer concentration in brain gray matter using positron emission tomography: MRI-based correction for partial volume effects", *Journal Cerebellum Blood Flow Metabolism*, vol. 12, pp. 571–583, 1992.
- [47] N. Ayache, P. Cinquin, I. Cohen, L. Cohen, F. Leitner, and O. Monga, "Segmentation of complex three dimensional medical objects: a challenge and a requirement for computer-assisted surgery planning and performance. In R. H. Taylor, S. Lavalley, G. C. Burdea, and R. Mosges, editors, *Computer integrated surgery: technology and clinical applications*, pp. 59–74, MIT Press, 1996.
- [48] W. E. L. Grimson, G. J. Ettinger, T. Kapur, M. E. Leventon, W. M. Wells, et al., "Utilizing segmented MRI data in image-guided surgery", *International Journal on Pattern Recognition and Artificial Intelligence*, vol. 11, pp. 1367–1397, 1997.
- [49] R. Jain et al, *Machine Vision*, McGraw-Hill, Inc. 1995.
- [50] M. Sonka, V. Hlavac, and R. Boyle, *Image Processing, Analysis, and Machine Vision*, Brooks / Cole Publishing Company, 1998.
- [51] S. W. Zucker, "Region growing: Childhood and adolescence", *Computer Graphics and Image Processing*, vol. 5, pp. 382-399, 1976.
- [52] L. J. Erasmus, D. Hurter, M. Naude, H. G. Kritzinger, and S. Acho, "A short overview of MRI artifacts", *SA Journal of Radiology*, vol. 8, no. 2, pp. 13-17, August, 2004.
- [53] M. Schmidt, I. Levner, R. Greiner, A. Murtha, and A. Bistriz, "Segmenting Brain Tumors using Alignment-Based Features", *IEEE 4th International Conference on Machine Learning and Applications, (ICMLA)*, pp. 215-220, December, 2005.

- [54] M. Sezgin, and B. Sankur, "Survey over image thresholding techniques and quantitative performance evaluation", *Journal of Electronic Imaging*, vol. 13, no. 1, pp. 146– 165, January, 2004.
- [55] M. Rastgarpour, and J. Shanbehzadeh, "Application of AI Techniques in Medical Image Segmentation and Novel Categorization of Available Methods and Tools", *Proceedings of the International Multi Conference of Engineers and Computer Scientists (IMECS) Hong Kong*, vol. I, March 16-18, 2011.
- [56] W. X. Kang, Q. Q. Yang, and R. R. Liang, "The Comparative Research on Image Segmentation Algorithms", *IEEE Conference on ETCS*, pp. 703-707, 2009.
- [57] L. Aurdal, "Image Segmentation beyond thresholding", Norsk Regnes central, 2006.
- [58] Wahba Marian, An Automated Modified Region Growing Technique for Prostate Segmentation in Trans Rectal Ultrasound Images, Master's Thesis, Department of Electrical and Computer Engineering, University of Waterloo, Waterloo, Ontario, Canada, 2008.
- [59] Y. Zhang, H. Qu, and Y. Wang, "Adaptive Image Segmentation Based on Fast Thresholding and Image Merging", *Artificial Reality and Tel-existence-Workshops*, pp. 308-311, 1994.
- [60] T. Lindeberg, and M. X. Li, "Segmentation and classification of edges using minimum description length approximation and complementary junction cues", *Computer Vision and Image Understanding*, vol. 67, no. 1, pp. 88-98, 1997.
- [61] H. Zhang, J. E. Fritts, and S. A. Goldman, "Image Segmentation Evaluation: A Survey of unsupervised methods", *Computer Vision and Image Understanding*, pp. 260-280, 2008.
- [62] H. G. Kaganami, and Z. Beij, "Region Based Detection versus Edge Detection", *IEEE Transactions on Intelligent Information Hiding and Multimedia Signal Processing*, pp. 1217- 1221, 2009.
- [63] Y. J. Zhang, "An Overview of Image and Video Segmentation in the last 40 years", *Proceedings of the 6th International Symposium on Signal Processing and Its Applications*, pp. 144-151, 2001.

- [64] Y. Chang, and X. Li, "Adaptive Image Region Growing", *IEEE Transaction on Image Processing*, vol. 3, no. 6, 1994.
- [65] K. K. Singh, and A. Singh, "A Study of Image Segmentation Algorithms for Different Types of Images", *International Journal of Computer Science Issues*, Vol. 7, Issue 5, 2010.
- [66] J. C. Bezdek, L.O. Hall, and L. P. Clarke, "Review of MR image segmentation techniques using pattern recognition", *Medical Physics*, vol. 20, pp. 1033–1048, 1993.
- [67] R. J. Schalkoff, *Pattern recognition: statistical, structural and neural approaches*, John Wiley and Sons, 1992.
- [68] A. P. Zijdenbos and B. M. Dawant, "Brain segmentation and white matter lesion detection in MR images", *Critical Reviews in Biomedical Engineering*, vol. 22, pp. 401–465, 1994.
- [69] T. Kapur, W. E. L. Grimson, R. Kikinis, and W. M. Wells, "Enhanced spatial priors for segmentation of magnetic resonance imagery", *In Proceeding of 1st International Conference on Medical Image Computational Component Assistant Intervention (MICCAI98)*, pp. 457–468, 1998.
- [70] J. W. Clark, "Neural network modeling", *Physics of Medicine and Biology*, vol. 36, pp. 1259–1317, 1991.
- [71] S. Haykin. *Neural networks: a comprehensive foundation*. Macmillan College, New York, 1994.
- [72] E. Gelenbe, Y. Feng, and K. R. R. Krishnan, "Neural network methods for volumetric magnetic resonance imaging of the human brain", *Proceeding of IEEE*, vol. 84, pp. 1488–1496, 1996.
- [73] W. E. Reddick, J. O. Glass, E. N. Cook, T. D. Elkin, and R. J. Deaton, "Automated segmentation and classification of multispectral magnetic resonance images of brain using artificial neural networks", *IEEE Transaction on Medical Imaging*, vol. 16, pp. 911–918, 1997.

- [74] A. P. Dempster, N. M. Laird, and D. B. Rubin, "Maximum Likelihood from in- Complete Data via the EM Algorithm", *Journal of the Royal Statistical Society: Series B*, vol. 39, no. 1, pp. 1–38, November, 1977.
- [75] R. C. Hardie, K. J. Barnard, and E. E. Armstrong, "Joint MAP registration and high-resolution image estimation using a sequence of under sampled images", *IEEE Transactions on Image Processing*, vol. 6, no. 12, pp. 1621–1633, December, 1997.
- [76] G. McLachlan and T. Krishnan. *The EM Algorithm and Extensions*. John Wiley & Sons, New York, 1996.
- [77] R. Ahmmed and, M. F. Hossain, "Tumor detection in brain MRI image using Template based K-means and Fuzzy C-means Clustering Algorithm", *Proceeding of 6th International Conference on Computer Communication and Informatics (ICCCI -2016)*, pp. 272-277, January 07 – 09, 2016, Coimbatore, INDIA.
- [78] R. Ahmmed and, M. F. Hossain, "Tumor stages detection in brain MRI image using Template based K-means and Fuzzy C-means Clustering Algorithm", *Proceeding of 11th Global Engineering, Science and Technology Conference*, pp. 1-10, 18 – 19 December, 2015, BIAM Foundation, Dhaka, Bangladesh.
- [79] (2015) PE- Brain tumor website. [Online]. Available: [http:// www.mayfieldclinic.com /](http://www.mayfieldclinic.com/)
- [80] University of Maryland Medical Center (2015) homepage. Primary brain tumor [Online]. Available: <http://umm.edu/health/medical/reports/articles/brain-tumors-primary>
- [81] Oncology (2015) homepage. Tumor type [Online]. Available: <http://www.oncolink.org/types/article.cfm?c=52&aid=247&id=9534>
- [82] X. Descombes, F. Kruggel, G. Wollny, and H. J. Gertz, "An object-based approach for detecting small brain lesions: Application to Virchow-robin spaces", *IEEE Transaction on Medical Imaging*, vol.23, no.2, pp.246–255, 2004.
- [83] J. Selvakumar, A. Lakshmi, and T. Arivoli, "Brain tumor segmentation and its area calculation in brain MR images using K-mean clustering and Fuzzy C-mean algorithm," *International Conference on Advances in Engineering, Science and Management (ICAESM)*, pp.186-190, 30-31 March, 2012.

- [84] B. N. Li, C. K. Chui, S. Chang, S. H. Ong, "Integrating spatial Fuzzy clustering with level set methods for automated medical image segmentation", *Computers in Biology and Medicine*, vol. 41, no. 1, pp. 1-10, 2011.

List of Publications

Conference Paper

- [1] R. Ahmmed and, M. F. Hossain, "Tumor detection in brain MRI image using Template based K-means and Fuzzy C-means Clustering Algorithm", *Proceeding of 6th International Conference on Computer Communication and Informatics (ICCCI -2016)*, pp. 272-277, January 07 – 09, 2016, Coimbatore, INDIA.
- [2] R. Ahmmed and, M. F. Hossain, "Tumor stages detection in brain MRI image using Template based K-means and Fuzzy C-means Clustering Algorithm", *Proceeding of 11th Global Engineering, Science and Technology Conference*, pp. 1-10, 18 – 19 December, 2015, BIAM Foundation, Dhaka, Bangladesh.